Mapping Coastal Habitats using an Imaging Spectrometer

by

Mark Zacharias
B.Sc., University of Victoria, 1991

A Thesis Submitted in Partial Fulfillment of the
Requirements for the Degree of

MASTER OF SCIENCE

in the Department of Geography

ACCEPTED
FACULTY OF GRADUATE STUDIES

[redacted]
DEAN

DATE 28 Apr 93

We accept this thesis as conforming
to the required standard

[redacted]
Dr. K.O. Niemann, Supervisor (Department of Geography)

[redacted]
Dr. D. Duffus, Departmental Member (Department of Geography)

[redacted]
Dr. A.P. Austin, Outside Member (Department of Biology)

[redacted]
Dr. G.A. Borstad, Outside Member

[redacted]
Dr. M.J. Whiticar, External Member

University of Victoria

Supervisor: Dr. K.O. Niemann

ABSTRACT

Airborne multispectral scanner imagery was acquired on Vancouver Island, British Columbia using an eight channel bandset configured for intertidal remote sensing. Radiance plots, between band correlations and a principle components analysis were used in the examination of two physically and biologically distinct littoral regions. Five of the eight bands were found to contribute significant unique information pertaining to intertidal vegetation and substrate identification. Classification of the resulting five bands demonstrated that different substrates and algal genera could be identified, including the differentiation of spectrally similar Chlorophytes (green algae).

Examiners:

[redacted]

Dr. K.O. Niemann, Supervisor (Department of Geography)

[redacted]

Dr. D. Duffus, Departmental Member (Department of Geography)

[redacted]

Dr. A.P. Austin, Outside Member (Department of Biology)

[redacted]

Dr. G.A. Borstad, Outside Member

[redacted]

Dr. M.J. Whiticar, External Member

ACKNOWLEDGMENTS

I would like to express my appreciation to the many people who contributed both time and funding towards this research. I would like to thank Drs. Olaf, Dave, Alan, and Gary for their co-operation and support, as well as Patrick Lucey for assistance in keying out specimens. Special thanks to Don Howes of the Ministry of Environment, Lands and Parks for funding data acquisition and to Richard Sykes for computer support.

Table of Contents

List of Tables

List of Figures

CHAPTER 1

INTRODUCTION

Intertidal (or littoral) environments comprise some of the most biologically productive regions on earth and are host to diverse assemblages of highly adapted flora and fauna. Human interference in these regions, however, often results in the loss of habitat for both the perennial and migratory species that utilize these areas (Bennett 1970, Carefoot 1983, Dickens *et al.* 1990, McConnaughey & McConnaughey 1986). As human population increases and societies industrialize, land near the ocean is often developed for residential, commercial, industrial or recreational use at the expense of natural habitats. Increasing human activities in coastal areas also results in increases in pollution in the form of domestic, industrial and agricultural wastes, as well as accidents such as chemical and oil spills (McConnaughey & McConnaughey 1986, Bennett 1970).

Only limited research has been undertaken upon the effects of human activities on coastal regions, as these areas have traditionally been perceived by North Americans as economically and ecologically less important than other resources (Bennett 1970, Wertheim 1984). The importance of coastal environments however, has increased in recent years due to a national and international demand for the products of these regions and a rise in public concern over the health of our coasts (Austin & Adams 1978, British Columbia 1990, Canada 1988).

One of the more prevalent concerns with respect to the coast of British Columbia is the threat of oil spills. The region's waters are frequented by tankers traveling from Alaska towards Washington State, resulting in elevated chances of a marine accident, such as the Exxon Valdez spill in 1989 (Dickens *et al.* 1990). According to Environment Canada, there were 574 marine spills in 1988, of which 22 were considered major, and 79% petroleum related. The number of spills in 1988 was a substantial increase over the 268 spills reported in 1984 (Canada 1991).

Concern over the consequences of a spill have been expressed by the local and national mainstream press, aboriginal groups as well as conservation and environmental organizations (*Kahtou*, Jan. 23 1989, *Maclean's*, Jan. 23 1989, Obee 1989, *Times Colonist,* Nov. 27 1992). The threat of a large B.C. oil spill was reinforced by both the Valdez spill and a spill resulting from a barge that sank on December 22, 1988 near the entrance of the Straight of Juan de Fuca (*Maclean's* Jan. 23 1989).

The Valdez accident provided valuable knowledge as to how spills affect coastal habitats and the success of various cleanup/recovery strategies. In a document examining the effectiveness and costs of different cleanup, containment and recovery programs, the U.S. Fish and Wildlife Service suggested that prior knowledge of the pre-spill plant and animal communities would have assisted in prioritizing cleanup efforts and minimizing costs. Knowledge of existing habitats may aid in managing cleanup efforts, as well as avoiding excessive costs of attending to species that may not be threatened (*Vancouver Sun*, Jan 4 1992).

Collecting information for coastal regions has traditionally been accomplished by fieldwork and a combination of airphoto interpretation and fieldwork. For intertidal and nearshore zones, aerial photographs are usually acquired and manually (visually) interpreted to identify different habitats (i.e. rock coasts or kelp beds). Intertidal regions can also be mapped using transects or, in the case of animal studies, marine life can be counted and populations estimated. Offshore coastal regions can be mapped using a variety of methods. Coastal circulation and bathymetry are normally determined by using current meters, tracking buoys and soundings. Primary production can be estimated using chlorophyll concentrations acquired *in situ* or more recently, satellite imagery (Pan *et al.* 1988).

These methods are labour intensive and costly, which may limit the amount and quality of information that can be collected (Austin & Adams 1978, Belsher *et al.* 1983, Hilton 1984, Lukens 1968, Sutherland 1989, Vadas & Manzer 1971). Satellite imagery

can be cost effective for examining coastal areas, but the spatial resolution (detail) and temporal resolution (frequency of coverage) of currently operational satellites are often inadequate for studying narrow coastal regions (Donoghue & Shennan 1987).

An alternative to aerial photographs and satellite imagery is the use of airborne digital sensors, also termed multispectral scanners or sensors (MSS) (Jensen 1986). These sensors allow the simultaneous acquisition of imagery in several spectral regions. Multispectral sensors are well suited to coastal imaging as they offer the advantages of aerial photographs and satellite imagery while eliminating some of the problems associated with these traditional methods. Digital imagery, once acquired, can be more cost effective than aerial photographs as imagery can be stored, analyzed and plotted using computers. The digital components of multispectral sensors also exhibit a greater spectral integrity and radiometric sensitivity than photographic dyes (Avery & Berlin 1992, Jensen 1986). When contrasted with satellite imagery, airborne systems allow a smaller area to be examined in detail, which is beneficial for certain narrow coastal regions (Avery & Berlin 1992).

Digital multispectral sensors have the potential to map and monitor many types of physical properties, communities, and phenomena. Physical properties include turbidity, water depth, terrestrial and submerged geologic formations, beach processes and sea surface temperatures (Bhargava & Mariam 1990, Borstad & Hill 1989, Hilton 1984). Biotic properties include locations and concentrations of intertidal and benthic algae (including kelps), phytoplankton, sea grasses, tidal pools and fish schools. Due to the low image acquisition costs of certain airborne sensors (compared with *in situ* fieldwork), imaging over several days may be economically feasible. As a result, natural phenomena such as algal blooms, upwellings, floods, fish schools, kelp forests and pollution (oil spills, industrial and domestic wastes, mine tailings, thermal pollution, forest siltation, etc.), may be monitored over time (Ardanuay *et al.* 1991, Borstad & Hill 1989, Maracci *et al.* 1990).

Data generated by airborne digital sensors also have the potential to be used as a planning tool, as coastal (foreshore) development can be periodically mapped. Advantages of multispectral techniques for this purpose are many. Aquaculture projects can be imaged to determine concentrations of both fish and pollution resulting from the farms (Kapetsky *et al.* 1987). Ocean log storage, and some of the detrimental effects associated with this practice, may be mapped as can oil leakage and spills from marinas and docks (Calabrese *et al.* 1987, Lockwood 1976). Charting the flow of wastes from mills and human settlements may lead to practical waste management schemes and an increased awareness of the effects of wastes on natural ecosystems (Zibordi *et al.* 1990).

With lightweight materials and advances in computer technology, multispectral sensors continue to offer better performance, lower initial purchase costs, and lower data acquisition costs since smaller aircraft are required (Borstad & Hill 1989). As a result, this technology continues to become an increasingly economically feasible alternative to aerial photographs and fieldwork.

The research reported in this thesis attempts to determine whether airborne multispectral data acquired using a new type of sensor, termed an imaging spectrometer, can be used to accurately map the vegetation and substrates in the intertidal and, to some extent, nearshore environments. If multispectral imagery can be accurately used to classify intertidal features, then habitat mapping using this technology may be feasible, which may result in a reliable and cost effective method of mapping coastal regions. The imaging spectrometer used in this study is termed the Compact Airborne Spectrographic Imager (CASI), and allows the user to tailor the spectral bandwidths of the instrument to the spectral properties of the physical and biological features under study. Consequently, part of this thesis is devoted to examining the spectral characteristics of the intertidal environment, and designing a bandset that allows insight into certain phenomena, or processes, that are only evident in certain narrow spectral ranges (i.e. chlorophyll fluorescence) (Neville & Gower 1977). Chapters one through three review previous

coastal remote sensing studies, and the physical, biological and chemical characteristics of intertidal and nearshore zones that effect the spectral properties of these regions. Chapter four discusses the methodology of the data collection and some of the problems encountered when remote sensing intertidal regions.

The remainder of this research involves acquiring the imagery using a bandset created for intertidal applications, and the evaluation, classification and accuracy assessment of the imagery. Chapter five will examine the spectral signatures of intertidal vegetation and substrates, and discuss their characteristics in light of the bandset used and signatures derived from other theoretical and applied studies. Chapter six will discuss the interrelationships between the bands using between band correlation matrices. Chapter seven applies a Principal Components Analyses (PCA) transformation to the imagery to highlight the spectral information pertaining to vegetation and substrate identification. The image data are classified in Chapter eight, and in Chapter nine accuracy assessment is applied to the classified images .

The conclusions presented in this research may be of value to those individuals and organizations interested in the possibility of using of airborne multispectral imagery for coastal mapping and monitoring. Using imaging spectrometers for intertidal remote sensing could be the first step in the creation of an extensive coastal inventory database, which would contain raw and classified imagery as well as ancillary data (any data that is not remotely sensed). Due to relatively low acquisition costs, imaging spectrometers could be used to periodically update areas of the database.

CHAPTER 2

THE REMOTE SENSING OF COASTAL ENVIRONMENTS

2.1. Introduction

This chapter will briefly trace the development of intertidal/coastal remote sensing from wartime applications during the early part of this century through the present day. Remotely sensed data may be acquired from airborne or spaceborne platforms, and can be collected in either analogue (photographs) or digital formats. This literature review will first discuss littoral remote sensing using photography, and then examine the digital methods that have been and are currently used.

2.2. Photographic Remote Sensing of Coastal Environments

Most photography used in the examination of the littoral environment has traditionally been acquired using aircraft, although certain early space explorations photographed coastal areas. The first remote sensing of coastal regions from space used photographs from the Apollo and Gemini space missions. Lepley (1968) concluded that Gemini photographs could be used in mapping coastal ocean areas, but suggested that future missions include a multispectral camera array designed for hydrological investigations. Kelly & Conrod (1969) also found that Gemini photographs could discern different vegetation types in areas of clear water, and concluded that higher resolution photographs from space would be much more beneficial (Kelly & Conrod 1969).

The use of aerial photography has been widespread in terrestrial studies since World War II, but has been infrequently used in the examination of the marine environment. One of the first documented uses of aerial photography for coastal research was the delineation and examination of submarine features during World War I (Lee 1922).

This technique was also used extensively in World War II for bathymetric studies (Kelly & Conrod 1969).

As early as 1950, aerial photos were used for identifying and mapping kelp beds (Cameron 1950), and by the early 1960's, remote sensing techniques had been applied to almost all aspects of the coastal marine environment. Many of the studies in the 1960's and 1970's concentrated on the north eastern coastal regions of the United States (Lukens 1968, Olson 1964).

2.2.1. *Comparisons of Film Types and Experimental Films*

During the last three decades, many papers have been published comparing the different film types (panchromatic, colour, false colour, and colour infared (CIR)) for the remote sensing of intertidal and marshland vegetation. These studies assessed the film types for water penetration, species and substrate identification, and the identification of mean high and low water marks. Some of the more prominent studies were undertaken by Austin & Adams 1978, Helgeson 1970, Lukens 1968, Olson 1964, and Specht *et al.* 1973.

One of the earliest projects was initiated by Olson (1964), in which he examined eleven types of vegetation in Maryland using two types of panchromatic film and two different color films. Photographs were acquired at 1: 5000, 1: 12000, and 1:20000 scales. To determine the optimum combination of film and scale, seven photointerpreters with varying levels of experience were asked to classify eight areas. Olson found that the type of film was not significant in species identification, but the scale of the photos, however, was very important in discriminating between different types (Olson 1964).

Lukens (1968) was involved in studying weed control measures for water chestnut in Chesapeake Bay, United States. Colour, CIR, and panchromatic films were used throughout August 1967 to determine the effectiveness of the weed control program. The

study found that colour and CIR films more accurately identified untreated weed areas than black and white photos. Color film was found to be the best film for detecting submerged weeds and identifying different species in the marine vegetation. The study also used infared imagery acquired both during the day and night to identify untreated areas, but it was found that there were no significant advantages in using infared imagery over conventional colour film (Lukens 1968).

Grimes & Hubbard (1971), used panchromatic, colour, and CIR films to identify vegetation on mudflats in Langstone Harbour, Southern England. Photographs were acquired throughout the year so that the optimum season for species identification could be determined. The study found that during February, March, May, and October, detail was more apparent on the panchromatic photographs. These monthly differences, however, may be attributed to hazy conditions during the flights (Grimes & Hubbard 1971). For the identification of non-vegetative features, color film was found to be slightly superior to panchromatic film. The study concluded that CIR film was superior to the other films, but often presented excessive detail which hindered the classification of large homogeneous areas. The only vegetation types that were more distinguishable on colour film than CIR were certain types of algae. The optimum month for differentiating between different vegetation types was found to be October as algal biomass peaked during this time (Grimes & Hubbard 1971).

Panchromatic, colour and CIR films were used in a seaweed survey undertaken by Jamison (1972). The study was initiated by the need to map commercially important beds of *Macrocystis* in order to locate and better manage the resource. Photographs were acquired in Washington State at 1:6000 scale using all three film types. The study found that colour film was most suited to subtidal surveys, while CIR was superior to colour film for intertidal remote sensing (Jamison 1972).

Several researchers and companies in the late 1960's began to realize the potential market for specialty films and filters that could penetrate water and discriminate between

submerged vegetation species. Experimentation with multispectral films and filters was evident as far back as 1950 (Cameron 1950), but no serious attempts at creating a new film for oceanographic remote sensing were made until the late 1960's (Helgeson 1970, Specht *et al.* 1973).

One approach proposed by Helgeson (1970) is the formulation of film dyes that detect reflectance in the blue-green and green regions of the spectrum, which most efficiently penetrate water. This contrasts with some of the other literature of the time that suggest removing the blue sensitive or yellow dye forming layer as it does not offer any significant water penetration capabilities (Lepley 1968, Currant 1969). According to Lepley (1968) and Currant (1969) the blue layer should be discarded in water penetrating films, as it was thought that haze and atmospheric scattering in the blue region would interfere with water penetration capabilities. According to Helgeson (1970), removal of the blue sensitive or yellow dye forming layer is unnecessary, rather the peak sensitivity of the dye should be moved to a region of the spectrum that is better suited for water penetration. The paper concludes that the spectral bands 430-530 nanometers (nm) and 540-620 nm are best suited for water penetration (Helgeson 1970). These results coincide with the findings of Yost & Wenderoth (1968), who concluded that both the green and blue bands are important for water penetration (Yost & Wenderoth 1968).

Another experimental film, designed by Specht *et al.* (1973) retained the blue sensitive layer as Helgeson (1970) suggested. Peak sensitivity of the film is in the regions of 480 nm and 550 nm with no red sensitivity, as red bands can obscure features at depth. A magenta dye was used for the blue-green sensitive layer, and a green dye was used in the green sensitive layer. When the film was tested, it was found that water penetration in open ocean water was greatest near 480 nm and water penetration in bays was better when the 550 nm band was used. The film also performed better than similar color films and color films with the blue sensitive layer removed (Specht *et al.* 1973).

Austin & Adams (1978) compared film types over the shores of Georgia Strait, British Columbia. The project used colour and CIR film to map the distributions of seaweeds along 80 km of the coastal intertidal region. Photographic data were acquired in 1972 and 1974, with ground truthing obtained in both years. Panchromatic, colour, and CIR films were initially used in the 1972 test flights, along with the experimental water penetration film discussed above (Specht *et al.* 1973).

Ground truthing was used to prepare 1:10000 seaweed vegetation maps that were used to assess the aerial photographs. Test photographs were acquired at 1:5000, and found that colour and CIR films were far superior to the panchromatic film, therefore black and white film was not used for the 1974 flights.

The study found that a combination of colour and CIR film yielded the best results as CIR film was useful in the identification of exposed algae but had poor water penetration capabilities, whereas colour film could penetrate up to seven meters below the surface but was not as efficient in identifying exposed vegetation. The experimental water penetration film (Specht *et al.* 1973) was found to be inferior to colour film for water penetration (Austin & Adams 1978).

Meulstee *et al.* (1988) used CIR photographs to determine a procedure for estimating biomass in the Oosterschelde Estuary, Netherlands. The study found that biomass could be reliably estimated using densitometric analyses of the photographs (Meulstee *et al.* 1988).

2.3. Satellite Remote Sensing of Coastal Areas

2.3.1. *The Landsat Series*

One of the first civilian digital multispectral satellites was the Landsat-1 (also called the Earth Resource Technology Satellite, or ERTS-1) which gathered data on the earth's

resources using the Return Beam Vidicon (RBV) and the four band Multispectral Scanner (MSS) sensors (Avery & Berlin 1992). The 80 m resolution of the MSS on Landsats 1-3 limited coastal remote sensing to only the larger estuaries and mud flats. Landsat 4 and 5 however, carried the Thematic Mapper (TM) which used 30 m pixels and seven spectral bands that were narrower and better suited to coastal studies than the MSS and RBV instruments (Table 2.1) (Budd & Milton 1982).

Table 2.1. Spectral Ranges for the Landsat Thematic Mapper (TM).

Band Number	Spectral Bands (nanometers)
Band 1	450 - 520
Band 2	520 - 600
Band 3	630 - 690
Band 4	760 - 900
Band 5	1550 - 1750
Band 6	10400 - 12500
Band 7	2080 - 2350

(Source: Jensen 1986).

2.3.2. *Early Landsat Thematic Mapper Simulations*

Prior to the launching of Landsats 4 and 5, several studies examined how the proposed Thematic Mapper bands could be used in estuarine, intertidal, and marshland studies. Budd & Milton (1982) used a portable radiometer to simulate the first four TM bands (blue to near infared, Table 2.1) for vegetation discrimination and biomass estimation in an intertidal marsh in southern England. The study attempted to map the distribution and amounts of *Spartina, Fucus, Zostera,* and *Enteromorpha.* The study concluded that identification of the four genera was possible using the proposed TM bands, but biomass estimation was not possible for *Spartina* and difficult for *Enteromorpha* (Budd & Milton 1982).

Hardisky *et al.* (1984) found that using a portable radiometer calibrated to the red and infared bands of the TM sensor (bands 3, 4, and 5), biomass estimates of *Spartina alterniflora* could be reliably predicted for several nearby marshes. The successful estimation of biomass in this study contrasts with the conclusions of Budd & Milton (1982) and may have been due to the use of red and middle infared bands, which could be used to discriminate between live and dead vegetation by detecting changes in chlorophyll and moisture content (Hardisky *et al.* 1984).

Populations of *Spartina anglica* were examined by Gross *et al.* (1985) using a hand held radiometer configured for TM bands 3, 4, and 5. Radiance measurements coupled with vegetation indices were used to predict *Spartina* biomass, where these predictions were later applied to four other separate marshes. The study found that biomass estimates using radiance data were accurate within 13 percent of actual biomass values in three of the marshes, but not accurate in the fourth marsh. Dead vegetation trapped in the live *Spartina* growth accounted for prediction errors in the fourth marsh (Gross *et al.* 1985).

Hobbs &Shennan (1986) used a four channel bandset configured to the first four TM bands in an attempt to determine the spectral separability of vegetation and sediment on the east coast of England. Measurements were collected using a four channel hand held radiometer configured to image 1 m squared pixels while ground truthing was performed at 1 m grid intervals throughout the study areas. Spectral data were clustered and classified using a) various clustering algorithms, b) a Principle Components Analyses (PCA), and c) a Two-Way Indicator Species Analysis (TWINSPAN). The study concluded that saltmarsh could be separated from non-saltmarsh and vegetated surfaces could be discerned from substrate surfaces. The study also found that certain species of vegetation could be identified by their spectral signature, and that the clustering techniques adequately discriminated between cover classes, but the PCA did not appear to contribute any new information to the clustered data (Hobbs & Shennan 1986).

2.3.4. *Coastal Thematic Mapper Studies*

One of the earliest Thematic Mapper estuarine studies was performed by Donoghue & Shennan (1987) using an image of the Wash Estuary in England. Bands selected for classification included band 2 for water penetration and vegetation reflectance; band 3 for its strong absorption by water and reflectance from substrates; band 4 for its water absorbance and infared reflectance from vegetation; and band 5 for detection of small moisture changes. A ratio of band 3/band 4 was substituted for band 2 as bands 2 and 3 were found to be strongly correlated. The image was classified using parallelepiped and maximum likelihood classifications, where upper marsh communities were poorly classified by both algorithms. The maximum likelihood classifier proved to be slightly more effective in separating spectrally similar vegetation and substrates in the mid to lower marsh communities. The study concluded that TM data could be used to accurately map larger marsh communities if current and reliable field measurements are obtained (Donoghue & Shennan 1987).

Subtidal coastal habitats in the western Arabian Gulf were mapped by Khan *et al.* (1992) using Thematic Mapper data. A PCA was applied to the water penetration bands (TM1 and TM2) so as to minimize the effects of changes in bottom depth, which resulted in the separation of five different subtidal habitats to a depth of 10 m (Khan *et al.* 1992).

Tassan (1992) used a Thematic Mapper image acquired over Venice Lagoon in 1989 to map occurrences of the green alga *Ulva rigida*, as increasing eutrophication of the lagoon has resulted in significant increases in algal populations, which interfere with human activities in the area. An algorithm was designed that, when applied to the image, differentiated between different depths of *Ulva* and does not require *in situ* measurements (Tassan 1992).

2.3.5. *Airborne Digital Multispectral Intertidal Remote Sensing*

Zibordi *et al.* (1990) used imagery acquired from the Airborne Thematic Mapper (ATM) to examine eutrophication in the Venice Lagoon. A Normalized Difference Vegetation Index (NDVI), was used which is given by;

$$NDVI = R(\lambda_2) - R(\lambda_1) / R(\lambda_2) + R(\lambda_1)$$

where R is reflectance at wavelength λ_i. The NDVI generally uses red and near infared (NIR) reflectances (<700 nm and >700 nm) to highlight vegetation as plants absorb strongly in the <700 nm ranges and reflect most of the radiation received in the >700 nm regions. The study concluded that by classifying a NDVI image with spectral bands centering on 660 and 830 nm, algal concentrations could be accurately mapped to a depth of approximately 50 cm (Zibordi *et al.* 1990).

2.4. Imaging Spectrometry

2.4.1. *Introduction*

The imaging spectrometer is the latest evolution in remote sensing technology. Its development resulted from a realization that traditional airphotos and satellite imagery lacked the spectral resolution to gain an in depth understanding of many objects and phenomenon. Sensors such as the Landsat Thematic Mapper, which has seven bands encompassing the visible and infared spectrum, are not able to detect differences between objects or phenomena if radiometric variations fall within one band of the sensor (Table 2.1). This lack of spectral resolution is particularly evident when attempting to discriminate

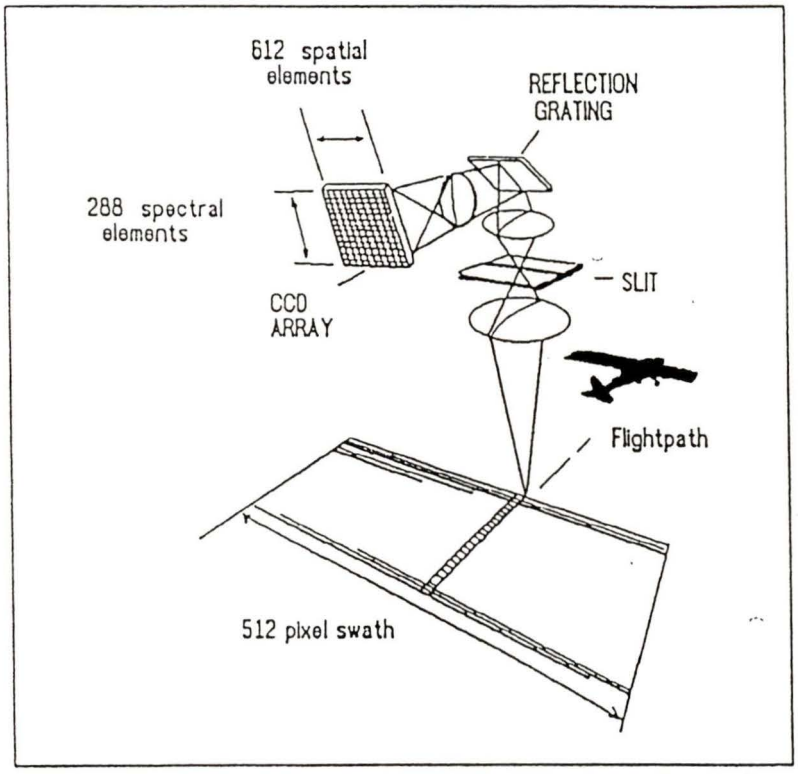

Figure 2.1 The components and operation of the Compact Airborne Spectrographic Imager (CASI). Most imaging spectrometers utilize the same basic design as the CASI (Borstad & Hill 1989).

between vegetation or geological features with similar spectral signatures (Kruse *et al.* 1990).

Imaging spectrometers are based on a Charge Coupled Device (CCD), which is an array of one or two dimensional elements, where each element in the array is a light sensitive diode (Chiu & Collins 1978). The CCD samples blocks of pixels where the number of pixels sampled depends on the number of array elements. The image is therefore acquired by the combination of the forward movement of the aircraft or satellite and the sampling of pixels across the swath of the array (Figure 2.1) (Borstad & Hill 1989).

As the CCD may be hundreds of pixels deep in the Y direction, the visible and infared spectrum can be separated into as many bands as there are elements in the Y direction of the array. As a result, spectral resolution is far superior than the traditional 4-7 bands available on current sensors (Table 2.2). There are several advantages of CCD technology over aerial photographs. First, spectral response of the array is linear and stable, whereas photographic dyes lack the spectral integrity and sensitivity to radiation that digital technology offers. Second, data acquired in digital format can be stored, manipulated and output using computers. Lastly, costs of CCD technology continue to decline, while accuracy and performance increase (Hodgson *et al.* 1981).

Prior to the development of the CCD, digital scanners used electromechanical optics in the form of a rotating mirror and detector. The disadvantages to this technology are a) mechanical systems are prone to failure, and b) the tolerances needed in the optics of electromechanical sensors are stringent, and sensors such as the Landsat TM have reached the limits of current design engineering practices. The next generation of research satellites is expected to have ground resolutions of as little as 10 meters square, and this cannot be accomplished using electromechanical methods (Thompson 1979).

A remote sensing device using a CCD is generally termed a "pushbroom" scanner, as the array sweeps along an area gathering an image as it passes. A fundamental

advantage of pushbroom technology over electromechanical devices is the lower integration time needed for the pushbroom scanner. A dwell period of 14 milliseconds is needed for the Landsat TM sensor, whereas only 12 milliseconds would be needed for a pushbroom sensor under identical conditions. This reduction in integration time yields a significantly better signal to noise ratio, and allows the optics of the system to be smaller and therefore lighter and less expensive (Thompson 1979).

Table 2.2. Imaging spectrometers currently available in North America, their year of construction, number of bands, spectral ranges and applications.

Sensor Name	Year	Bands	Range (nm)	Applications
Chiu and Collins Spectroradiometer	1976	500	400-1100	research
Linear Array Pushbroom Radiometer	1978	13	400-1000	research
Airborne Imaging Spectrometer	1981	128	1200-2400	research-geological
Fluorescence Line Imager	1981	288	430-800	marine mapping
Airborne Visible & Infared Imaging Spectrometer	1988	224	410-2450	research
Geophysical and Environmental Research Imaging Spectrometer	1989	63	400-2500	commercial-geology
Compact Airborne Spectrographic Imager	1989	288	425-950	commercial-forestry/marine

(Sources: Borstad *et al.* 1985, Borstad & Hill 1989, Chiu & Collins 1978, Kruse *et al. 1990,* Porter & Enmark 1987)

Another advantage of the pushbroom scanner is the availability of commercial and industrial CCD's compared to the costly designing and construction of electromechanical optics (Hodgson *et al.* 1981). A disadvantage of the CCD compared to other imaging methods is that the array must be calibrated, which can require two to three weeks and several thousand dollars (CDN) (G.A. Borstad, personal communication). CCD technology is also limited by the inability of the array to detect middle and long wave infared reflectance. This problem will probably be remedied in the near future (Avery & Berlin 1992).

2.4.2. *The Columbia University Spectroradiometer*

Although the Jet Propulsion Laboratory in California claims to have produced the first operational imaging spectrometer with the Airborne Imaging Spectrometer (AIS), the first imaging spectrometer was constructed at Columbia University (Chiu & Collins 1978, Avery & Berlin 1992, and Vane *et al.* 1984).

The Columbia University imaging spectroradiometer was not named, but often termed the Chiu and Collins spectroradiometer (Chiu & Collins 1978). It was initially flown in 1976 and continued to be used for several years. The system could detect in the 400-1100 nm regions of the spectrum using 500 bands (channels) and could be mounted in a small twin engine aircraft. At 200 km/h flying at 600 meters, pixels were 18 meters square (Chiu & Collins 1978).

The system was flown over several different targets to assess its performance for different types of remote sensing studies. Data were acquired in the Goldfield, Nevada area for mapping hydrothermal alteration products, which are often indicators of heavy mineral deposits. It was found that limonite, hematite, and jarosite could be discerned using the sensor. The sensor was also successful in differentiating between wheat at various stages of growth and could identify areas of stressed forest growing over sulfide mineral deposits. Lastly the scanner was successful in identifying zones of different algae in two California lakes (Chiu & Collins 1978).

The spectroradiometer was also tested by the U.S. Army Corps of Engineers for water quality monitoring in lakes, reservoirs, and waterways (McKim *et al.* 1984). The study concluded that the sensor could detect sediment loads to an accuracy of 5 ppm. The study also found that different types of sediments exhibited different spectral characteristics, but no work was performed on the identification of these sediments using the instrument (McKim *et al.* 1984).

2.4.3. *The Linear Array Pushbroom Radiometer*

An experimental imaging spectrometer was constructed by the NASA Goddard Space Flight Centre in 1978 (Hodgson *et al.* 1981). Called the Linear Array Pushbroom Radiometer (LAPR), it consists of three 512 diode linear arrays which are sensitive to radiation from 400 to 1000 nm. The LAPR was the first imaging spectrometer to incorporate roll correction information in the geometric correction of the images. The sensor was used for detecting moth defoliation of forests and coal strip mining practices in Pennsylvania. The study found that the sensor could identify areas of moth defoliage as well as delineate mined areas and areas at different stages of reclamation. The only apparent disadvantage to the LAPR is a fair amount of striping or banding that occurs due to the inability of the array to be properly calibrated (Hodgson *et al.* 1981).

2.4.4. *The Airborne Imaging Spectrometer*

The Airborne Imaging Spectrometer (AIS) uses a 32 by 32 element mercury cadmium telluride (HgCdTe) array and was designed to assess the ability of imaging spectrometers to detect in the infared regions of the spectrum. The instrument uses 9.3 nm bands ranging from 1200 nm to 2400 nm, which yields scenes that are 32 pixels wide and comprise 128 bands (Vane *et al.* 1984). Pixels are 8 meters square when flown at an altitude of 4200 meters. The AIS was flown from 1984 to 1986 on a Hercules C-130 aircraft (Kruse *et al.* 1990).

As with the Chiu & Collins spectroradiometer, the AIS was tested on hydrothermally altered rocks in Nevada, which found that the sensor could detect kaolinite and alunite bearing samples. The AIS was also assessed for vegetation identification by comparing results from the sensor with a simulated Landsat TM image and CIR photography. The study found that high spectral resolution in the 1200 to 1500 nm region

of the spectrum was better suited to vegetation identification than several wide bands throughout the visible and infared spectrum (Vane *et al.* 1985).

2.4.5. *The Fluorescence Line Imager*

The first Canadian imaging spectrometer was constructed in 1981 by Moniteq Ltd. of Toronto and Itres Ltd. of Calgary under contract from the Department of Fisheries and Oceans (DFO). The DFO was interested in mapping surface phytoplankton in coastal areas as it constitutes the primary level in the marine food chain, and can therefore be used as an indicator of primary productivity (Borstad *et al.* 1985, Fogg & Thake 1987). Termed the Fluorescence Line Imager (FLI), the sensor was also designed to assist in hydrographic mapping, water quality monitoring, and mapping of bottom features (Borstad *et al.* 1985).

The FLI uses five CCD's, each combined with a camera in a separate housing. Each detector can sample 385 spatial pixels for a total of 1925 spatial pixels, while 288 spectral pixels are available. Spectral resolution is 2.5 nm and can be selected in increments of 1.4 nm within a range of 430 to 800 nm (Borstad *et al.* 1985). Its major weaknesses are the inability to detect radiation above 850 nm, difficulty in calibrating the instrument, and excessive sensor weight (Borstad & Hill 1989).

The FLI was used in 1985 to examine forest damage in Vermont and West Germany. The health of spruce and fir forests in both the U.S. and Germany has decreased throughout the past several decades. These changes are thought to be due to increases in pollution in the form of acid rain, ozone, and heavy metals (Rock *et al.* 1988). Stressed vegetation can be identified by a 5 nm shift (approximately) of the average red edge reflectance toward the shorter (blue) regions of the spectrum. This shift is caused by a reduction in chlorophylls within the needle leaves of the trees.

The Vermont site was imaged in 1985 using the FLI and results were compared with the *in situ* Visible Infared Intelligent Spectrometer (VIRIS). The study concluded that

the FLI could detect subtle changes between different types of chlorophylls and carotenoids, but was not able to differentiate between natural mortality and stress due to pollution (Rock *et al.* 1988).

The FLI has also been used in the detection and mapping of phytoplankton (Gower & Borstad 1990). Chlorophyll *a* absorbs light in the 450 nm region and fluoresces within a narrow band centered around 685 nm. The presence of phytoplankton (and therefore chlorophyll *a*) will tint the surface of a water body green due to absorption near 450 nm and higher backscatter between 500 and 600 nm. The FLI was flown over Barkley Sound, British Columbia where it was able to successfully detect and map concentrations of phytoplankton with a greater accuracy than airphoto interpretation or the human eye. Successful detection of the organisms depended on the use of chlorophyll *a* fluorescence characteristics of the phytoplankton rather than ocean colour changes between 500 and 600 nm (Gower & Borstad 1990).

2.4.6. *The Airborne Visible and Infared Imaging Spectrometer*

The Airborne Visible and Infared Imaging Spectrometer (AVIRIS) is a second generation sensor based on the AIS and was first used in 1988. The sensor utilizes 10 nm bands (224) ranging from 410 to 2450 nm, and is flown at an altitude of 20 km. Pixels measure 20x20 m over a 10 km swath. The AVIRIS uses four spectrometers to gather the 224 bands and weighs 327 kg (Porter & Enmark 1987).

2.4.7. *The Geophysical and Environmental Research Imaging Spectrometer*

The Geophysical and Environmental Research Imaging Spectrometer (GERIS) was designed by the Geophysical Research Corporation (U.S.) for commercial applications

(Kruse *et al.* 1990). The sensor detects reflected radiation in 63 variable width bands ranging from 400 to 2500 nm, and includes a separate 64th band for aircraft attitude information. The system is mounted on a small twin engine aircraft and generally flown at 6000 meters (Kruse *et al.* 1990).

As with several other imaging spectrometers discussed previously, the GERIS was flown over the Cuprite mining district of Nevada. The study found that the GERIS could easily identify mineral deposits that were difficult to locate using ground surveys. The data quality of the GERIS represented a significant improvement over data acquired from the AIS and Chiu & Collins spectroradiometer (Kruse *et al.* 1990).

2.4.8. *The Compact Airborne Spectrographic Imager*

The Compact Airborne Spectrographic Imager (CASI) was constructed in 1988 by Itres Ltd. of Calgary as an improvement on the Fluorescence Line Imager. The major differences between the FLI and the CASI are the greater flexibility of spectral and spatial bands with the CASI, the use of only one CCD rather than five, the use of digital cassette tape as a storage medium, and a greatly reduced sensor weight (Borstad & Hill 1989).

The CASI can operate in what is termed either spectral or spatial mode, where the bandwidths and spectral resolution are user defined. In spectral mode, each along-track column of the CCD acts as a separate spectrometer with a 1.8 nm resolution from 425 to 950 nm. As it is not currently feasible to write data from 512 separate spectrometers onto magnetic media at a rate that matches forward velocity, the CASI limits the number of spectral columns to 39. The width and placement of these columns along the swath of the image is user defined. To aid in the interpretation and understanding of the data, a "track-recovery" image is supplied with the spectral image. This is a high resolution monochromatic spatial image that is sampled along with the spectral data. The track recovery image spectral wavelength is selected by the user. Spectral data are acquired in a

12 bit format (padded to 16 bit format) resulting in up to 4096 brightness values (Borstad & Hill 1989).

The CASI spatial image is 512 pixels wide for use in smaller image processing systems and has user programmable bandwidths that can be as narrow as 1.8 nm. The spectral range for spatial imaging ranges from 426 to 946 nm and up to 15 bands can be placed at any point within this region. Use of more than 15 bands (approximately) results in excessively large pixels in the along-track direction. At a flight altitude of 2000 meters and traveling at 100 kts, pixels measure 2.4 m in the cross track direction and 2.5 m in the along track direction. Data are written either in 8 or 16 bit format (Borstad & Hill 1989).

The CASI data are collected on 8mm videotape which can contain up to 1.1 gigabytes of digital data, or about 1 hour of flight time. The data are extracted by custom software (Borstad Associates Ltd.) and transferred to a PC hard disk or other storage medium. As its name suggests, the CASI is very light compared to other multispectral scanners. In total the CASI weighs only 55 kg, compared to 137 kg for the FLI (Borstad & Hill 1989).

The CASI was used in 1989 to map chlorophyll and ocean pollution in Norway (Pettersson *et al.* 1990). It was found that the sensor could determine chlorophyll *a* concentrations in surface water, but could benefit from a better method of atmospheric correction (Pettersson *et al.* 1990). The CASI has also been applied to fish detection and monitoring terrestrial and marine vegetation (Borstad & Hill 1990).

2.4.9. *The Future of Imaging Spectrometry*

The next generation of U.S. Earth Observation Satellites (EOS) will be fitted with several types of imaging spectrometers. One proposed system is termed the High Resolution Imaging Spectrometer (HIRIS), which will collect spectral data at 10 nm intervals within the 400 to 2500 nm region of the spectrum using 30 metre square pixels

(Goetz & Herring 1989). Another proposed sensor is the Moderate Resolution Imaging Spectrometer (MODIS), which will be used to complement the HIRIS. The MODIS will be a fixed sensor aiming directly below the platform, and will use 36 spectral bands (Ardanuay *et al.* 1991). Both sensors will have a 410 to 875 nm spectral resolution and pixel sizes will vary from 250 to 1000 meters (Ardanuay *et al.* 1991).

Other sensors under development include the Advanced Spaceborne Thermal Emission and Reflection Radiometer (ASTER) for the Japanese government, the Digital Airborne Imaging Spectrometers (DASI) for the European Space program and the commercially orientated Multispectral Infared and Visible Imaging Spectrometer (MIVIS) by Daedalus Enterprises of the U.S (Staenz 1992). The newest sensor nearest to operational capability, however is NASA's Advanced Solid-State Array Spectroradiometer (ASAS), which operates in the 455 nm - 873 nm regions using 29 bands. The ASAS is currently undergoing operational testing for future airborne and spaceborne applications (Ardanuay *et al.* 1991, Staenz 1992)

CHAPTER 3

THE INTERTIDAL AND NEARSHORE ENVIRONMENTS

3.1. An Introduction to Intertidal and Nearshore Environments

The intertidal, or littoral zone, is the meeting place of the terrestrial and marine environments. The result of this meeting is an "edge" area that is subjected to the influences of both these environments, and as a result, becomes host to a wide variety of habitats which are noted for their rich diversity of organisms (Carefoot 1983).

All intertidal shores, no matter how large or small the tidal range, have some degree of zonation or banding of the organisms that exist on them. Just as plant communities on mountains occupy definite bands or zones corresponding mainly to the tolerance of decreasing temperature with increasing elevation, so intertidal communities occupy definite zones on the shore. However, in comparison, the zones that occur in the intertidal environment are very much compressed vertically and are subject to a number of different biophysical factors (Carefoot 1983, Dethier 1982, Hruby 1976).

The zonation of littoral environments is a result of the varying responses of the marine organisms to environmental factors that are related directly or indirectly to the tidal cycle. The upper limits of these zones are created by the organism's tolerance to physical stresses associated with a lack of water. They include desiccation, temperature extremes, lack of oxygen and lack of food. The lower boundary of these zones is determined by the organism's ability to deal with biological stresses such as the competition for space, resources, and in the case of marine plant species, light and herbivory (Carefoot 1983, Dethier 1981, Hruby 1976).

The size and species composition of these zones is determined by the above environmental conditions as well as the tidal range of the shore, the shore slope, and the physical makeup of the shore. Generally, where the range of the tides is small and/or the

slope of the beach is steep, the zones are narrow. Conversely, where the tidal range is great and/or the slope of the beach is gradual, the zones are wide. The physical makeup of the shore, as well as its geographical location, determines the types of organisms that occur there. For example, clams are found on sandy or muddy beaches where they can bury into the sediments. This protection is not offered on rocky shorelines, and as a result few clams are found on them (Carefoot 1983, Kozloff 1983).

The British Columbia coast can be classified using several physical indicators, which include temperature, salinity, pressure, light intensity and the amount of energy transferred to the shore as a result of waves, tides and currents. As wave and tidal processes tend to be the most influential factors in shaping the physical and biological characteristics of the shore, for this discussion shorelines can be separated into three categories; a) exposed, b) protected, and c) transitional shores (Odum 1989). These three categories can be further subdivided into the characteristic shore types that occur within them (Snively 1983).

Exposed shorelines are located along unprotected areas of the outer coast, where they are subjected to the full force of the Pacific Ocean surf (Snively 1983). The two physical shore types found in these areas are composed mainly of rock or sand (Kozloff 1983, McConnaughey & McConnaughey 1986). The majority of the intertidal organisms can be found on rocky shores where they can find attachment and are not subject to the scouring action which occurs in sand or gravel environments (Snively 1983). Exposed rocky shores support a highly specialized but limited variety of organisms that are adapted to withstand the extreme conditions. The adaptations of these surf-dwelling organisms include strong attachment devices, reduced surface area, protective clustering behavior, the use of micro habitats such as tide pools and crevices for protection and, in the case of seaweeds, a "woody" texture or heavy integument (Carefoot 1983, Moore & Seed 1986).

On rocky exposed shores the splashing of the waves permits organisms to exist higher on the shore than they would normally. This affects the overall width of the

intertidal region. The increased wave exposure also makes the upper and lower boundaries of the zones less distinct (Carefoot 1983, McConnaughey & McConnaughey 1986, Moore & Seed 1986). The invertebrate species that occur in this region include colonies of *Mytilus calfiornianus* Linnaeus, *Pollicipes polymerus* Conrad, *Thais canaliculata* and *Collisella digitalis* . Seaweeds adapted to these surf conditions include the brown algae *Laminaria setchellii* Silva, *Lessoniopsis littoralis* Reinke, *Hedophyllum sessile* C. Agardh, and *Postelsia palmaeformis* Ruprecht (Carefoot 1983, Kozloff 1983, McConnaughey & McConnaughey 1986, Moore & Seed 1986, Scagel 1961).

The protected shores of British Columbia are sheltered by offshore islands or are located in inlets, bays and straits which protect them from heavy wave exposure (Snively 1983, McConnaughey & McConnaughey 1986). As a result they are host to habitats which could not exist on the outer coast. These habitats include shore types such as rocky out-crops, beaches composed of cobblestones or gravel, and at the low tide line, sand and mud flats. Estuaries and salt marshes are also major habitats of this region (Kozloff 1983, McConnaughey & McConnaughey 1986).

On the protected beaches, organisms occur in zones smaller than those found on the rocky outer coasts. The most distinctive zonation is associated with shorelines composed of rock outcrops and/or large cobble or boulder sized stones (Snively 1983). In these intertidal areas, some of the more common species of invertebrates include *Mytilus edulis* Linnaeus, *Thais lamellosa* Gmelin, *Polinices lewisii* Gould, *Anthopleura xanthogrammica* and *Pisaster ochraceus* Brandt. The more prevalent algal species which are found in these areas include *Fucus distichus* Gardner, *Ulva lactuca* Linnaeus, *Laminaria saccharina* Linnaeus, *Iridaea cordata* Turner, *Alaria marginata* Postels and Ruprecht, *Gigartina exasperata* Harvey and Bailey, *Enteromorpha spp.* Linnaeus and *Corallina spp.* Harvey (Kozloff 1983, McConnaughey & McConnaughey 1986, Scagel 1961).

Transitional shores along the coast of British Columbia are subject to a degree of wave exposure that lies somewhere between that experienced by exposed and protected

shores (Snively 1983). The physical make-up of the intertidal zone is very similar to that found on exposed shorelines. The biological communities that occur in these two areas, however, are quite different, largely a result of differing degrees of wave exposure. The organisms found on transitional shores are adapted to the variety of exposure conditions and, as a result, they can also be found on protected or exposed intertidal areas (Kozloff 1983, McConnaughey & McConnaughey 1986). As with exposed littoral regions, the sand and gravel beaches of transitional areas are typically sterile, a result of the scouring action of the sediments (Snively 1983). Most of the marine organisms in transitional intertidal habitats are found on the rocky areas. They include the marine plants *Phyllospadix spp.* Hooker, *Corallina spp., Iridaea cordata, Egregia menziesii* Turner and *Alaria marginata.* Prolific sessile marine invertebrates found on these shores include *Mytilus californianus, Pollicipes polymerus* and various other barnacle species (Kozloff 1983, McConnaughey & McConnaughey 1986, Scagel 1961).

3.2. An Introduction to the Algae

The most abundant photosynthetic organisms in the intertidal and nearshore environments are the algae, or seaweeds. Disagreement exists in the biological community as to the definition of "algae", but the term generally encompasses almost all thallophytes (with the exception of certain genera), which are plants that lack roots, stems, and leaves, and in which chlorophyll *a* is the dominant photosynthetic pigment (Campbell 1987, Lee 1989). Algae are also distinguished from higher plants by the absence of a multicellular wall surrounding the sporangia or gametangia (reproductive cells) (Bold & Wynne 1978, Lee 1989). The term "algae" is quite broad, therefore organisms considered to be algae range from the unicellular blue - green algae, which are closely related to bacteria, to the very large and complex marine macroalgae (seaweeds), which resemble terrestrial vascular plants by exhibiting stem and leaf-like structures (Lee 1989).

Algae occur in both freshwater or marine environments, although many species may reside in soils, snowpacks, hot springs, or in conjunction with fungi to create lichens (Bold & Wynne 1978, Campbell 1987, Lee 1989).

3.3. Characteristics of Marine Algae

Marine macroalgae, or seaweeds are those species where an individual organism can be seen with the naked eye (Bold & Wynne 1978). Macroalgae dominate the intertidal zone, and are evident as patches of different colored vegetation. Marine macroalgae can be differentiated into three classes according to their colour. Green algae are part of the class Chlorophyceae, brown algae the Phaeophyceae, and red algae fall within class Rhodophyceae. The different colours are a result of different types and amounts of photosynthetic pigments utilized by the organism. All eukaryotic photosynthetic organisms contain chlorophylls, but the characteristic green appearance of the chlorophylls is often masked by the presence of brown pigments termed carotenoids, or several types of red and blue pigments known as biliproteins. Certain carotenoids and all biliproteins are termed accessory pigments, as their function is generally thought to assist the chlorophylls in the harvesting light energy by collecting light in spectral ranges outside the wavelengths utilized by the chlorophylls (Bold & Wynne 1978, Kirk 1983, Lee 1989, Rowan 1989, Scagel 1967).

Marine macroalgae exhibit a wise range of morphologies, depending upon the species and the reproductive phase. As the macroalgae are multicellular and non-motile, the structure of the organism is generally a) filamentous, b) membranous or foliar, c) tubular, d) blade-like, or e) leafy (Bold & Wynne 1978, Lee 1989).

3.4. Spectral Properties of the Algae

In photosynthetic organisms, light is harvested by certain pigments and combinations of pigments. These pigments include the chlorophylls (*a*, *b*, c_1, c_2, and *d*), some of the 400 variations of carotenoids, and biliproteins (phycocyanin, phycoerythrin, allophycocyanin and phycoerythrocyanin) (Kirk 1983, Lee 1989, Rowan 1989). Within each species, photosynthesizing cells in structures termed chloroplasts contain a mixture of different pigments, where the type of pigments present and the ratios of the various pigments are specific to certain species at certain locations and times (Ramus & Rosenberg 1980, Rowan 1989). As light interacts with these pigments, it is either absorbed, reflected, or altered depending on the quantity and ratio of the photochemicals and the shape, size, and structure of the cell (Kirk 1983, Lee 1989, Rowan 1989). Altered light is often exhibited in the form of fluorescence, where light of one wavelength is absorbed and reflected out of the cell as light of another wavelength (Neville & Gower 1977). Spectral characteristics of the cell may be altered depending on whether it is part of a colony, and the size, shape, and thickness of the group of cells (Lee 1989). Previous research has shown that it is possible to identify certain species using their spectral properties, if the amounts and ratios of the photosynthetic pigments are known *a priori* (Kirk 1983, Lee 1989, Ramus 1981, Rowan 1989).

The measured absorption/reflectance/fluorescence characteristics of seaweeds and sea grasses in their natural habitats may change significantly from these characteristics measured under laboratory conditions. This is due to several factors. First, laboratory studies may determine the absorption spectra of an alga where the thylakoids (structures containing pigments) are not arranged in their natural fashion, and therefore collect light differently in the laboratory than *in situ* (Kirk 1983, Rowan 1989). Second, pigments are extracted from vegetation using solvents, which can shift peak absorption areas towards the red or the blue ends of the spectrum (Ramus & Rosenberg 1980, Rowan 1989). Third,

spectral characteristics measured in the laboratory do not consider the effects of density and community structure, and the presence of other vegetation which may naturally occur in conjunction with the alga under study (Lee 1989, Rowan 1989). Fourth, some algae can adapt to suit the antecedent light conditions by varying the amount and type of pigments produced. This phenomenon is termed chromatic adaptation (Lee 1989). Consequently, one species that exists in clear water may contain different types and ratios of pigments than the same species living in a highly turbid region (Kirk 1983, Ramus 1981, Rowan 1989).

3.5. Photosynthetic Pigments of the Algae

Algae inherit their characteristic red, green, and brown colours from mixtures of three different types of photosynthetic pigments. These pigments, termed the chlorophylls, carotenoids and biliproteins are responsible for the conversion of solar energy into chemical energy (Kirk 1983). All photosynthetic eukaryotic plants contain chlorophylls, but the presence of carotenoids and biliproteins give the different groups of algae their different colours (Campbell 1987).

3.5.1. *The Chlorophylls*

The most widely occurring pigments are the chlorophylls, which are present in various forms in all photosynthetic eukaryotic organisms. The most abundant type of chlorophyll, chlorophyll *a*, is utilized by all photosynthetic eukaryotic organisms, while the presence of chlorophylls *b*, c_1 and c_2, and *d* is group/division dependent. The type and quantity of chlorophylls present are important systematic indicators and their spectral properties can be used to differentiate between groups of algae (Figures 3.2 & 3.3) (Kirk 1983, Lee 1989, Rowan 1989).

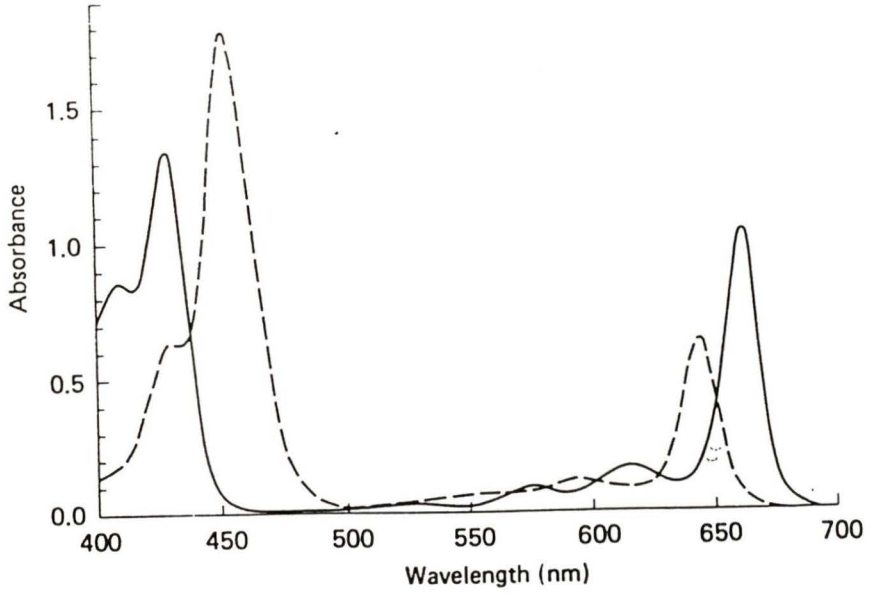

Figure 3.2. The absorption spectra of Chlorophylls *a* and *b* determined in the laboratory using diethyl ether as a solvent (after French 1960, Kirk 1983, Rowan 1989) (Chlorophyll *a* _____, Chlorophyll *b* -------).

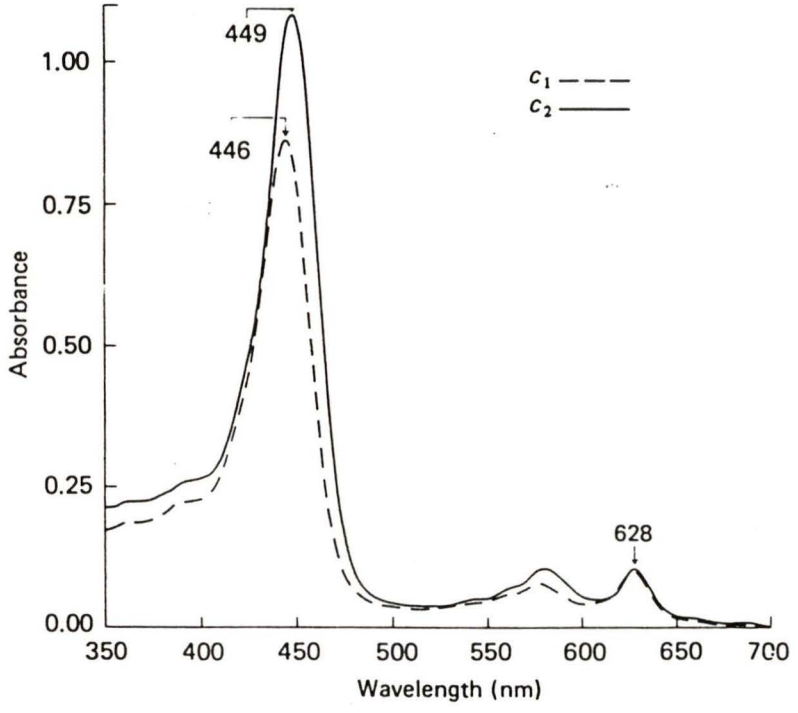

Figure 3.3. The absorption spectra of Chlorophyll c1 and c2 determined in the laboratory using acetone as a solvent (Kirk 1983) (Chlorophyll c1 ---------, Chlorophyll c2 _____).

Chlorophyll *a* absorbs blue and red light in the 430 nanometre (nm) and 660 nm range respectively, and fluoresces near 685 nm (Rowan 1989). The amount of chlorophyll *a* fluctuates widely depending on the class, genera and species. In a study performed by Egle (1960) in Scandinavia, red algae were found to contain 0.09-0.44 percent chlorophyll *a* by weight while, brown and green algae contained 0.17-0.55 percent and 0.28-1.53 percent respectively (Egle 1960, Kirk 1983, Rowan 1989). Chlorophyll *b* is chemically similar to chlorophyll *a* but absorbs light near the 460 nm and 640 nm regions of the spectrum and fluoresces near 650 nm. Chlorophyll *b* is generally less abundant than chlorophyll *a* and has been found to occur in approximately 1/3 ratios (chlorophyll *a*/*b*) for fresh water green algae and 1/1 -1/2.3 ratios for marine green algae (Kirk 1983). In the algae, chlorophyll *b* is present only in the Chlorophyta, Euglenophyta, Prasinophyta and Prochlorophyta groups, thus serving as an important indicator of systematic relationship (Lee 1989).

Chlorophylls c_1 and c_2 are present in the Chrysophceae (golden-brown algae), Bacillariophyceae (diatoms), and Phaeophyta with c_2 present only in the Pyrrophyta and Cryptophyta. Chlorophyll *c* is present in similar ratios of chlorophyll *a* to *b* (1/3). Absorbance for chlorophyll *c* is between 445 and 450 nm, with small absorbance peaks at 570 nm and 628 nm. Chlorophyll *c* fluoresces near 635 nm (Kirk 1983, Rowan 1989).

Chlorophyll *d* is chemically very similar to chlorophyll *a*, but has a unique spectral signature. The pigment absorbs in the 445 nm and 696 nm range and is found only in some species of red algae, usually in small quantities (Rowan 1989).

3.5.2. *The Carotenoids*

Unlike the chlorophylls, the 400 plus types of carotenoids are present in both animals and plants. Whereas the chlorophylls have the singular task of converting light into chemical energy, the carotenoids perform many roles depending on the organism and

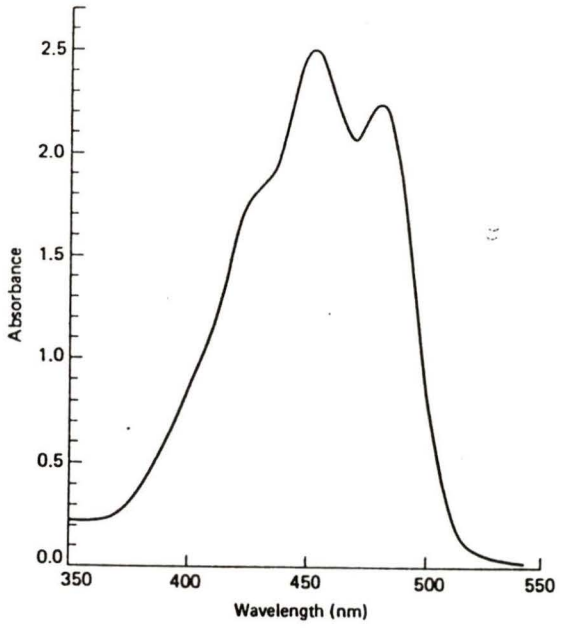

Figure 3.4. The absorption spectrum of *B* - carotene. Each carotenoid has a unique spectral signature, but all have the characteristic high reflectance in the 500 nm regions (Kirk 1983).

the parameters of its environment. These pigments may convert green, yellow, or yellow-red light into wavelengths that can be used by the chlorophylls, or they may protect the organism from excessive insolation (Kirk 1983, Rowan 1989).

Carotenoids absorb longer wavelength radiation (450-560 nm) near the blue end of the spectrum than do the chlorophylls which give organisms containing the pigment a brownish-orange color (Figure 3.4). The weight ratio of carotenoid to chlorophyll differs according to species, but has been found to be 1/0.5 in *Laminaria* and 1/2 in *Hormosira* (Kirk 1983, Rowan 1989).

3.5.3. *The Biliproteins*

The biliproteins are found only in the Rhodophyta, Cryptophyta and Cyanophyta. They are separated into two main groups, algae with phycobilisomes (Cyanophyceae, Rhodophyceae) and algae without (Cryptophyceae). Phycobilisomes are granular particles of biliproteins situated on the thylakoids. Their function has not been positively determined, but it is thought that they may be used to direct light energy into the thylakoids (Campbell 1987). The biliproteins can be of two colours; blue and red where phycocyanins and allophycocyanins comprise the blue, and phycoerythrins and phycoerythrocyanins comprise the red (Figure 3.5). The maximum absorbance peak is characterized by a red shift from phycoerythrins through phycocyanins and allophycocyanins. All blue-green and red algae contain phycocyanins and allophycocyanins but phycoerythrins (phycoerythrocyanin) are not always present, especially in blue-green algae.

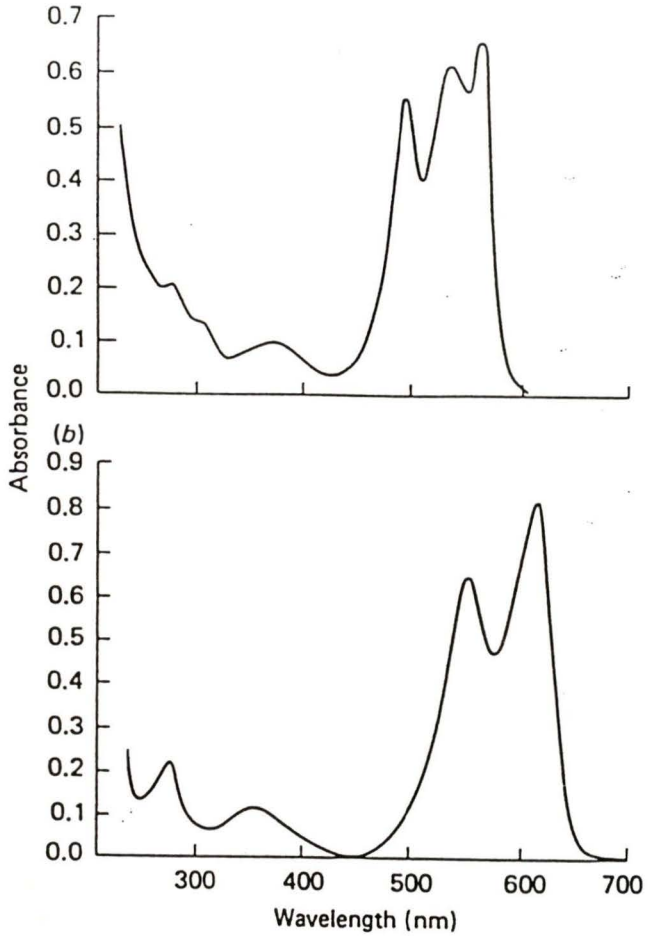

Figure 3.5. The absorption spectrum of the biliproteins R-phycoerythrin from *Ceramium rubrum* (a) and R-phycocyanin from *Porphyra laciniata* (b) (Kirk 1983).

CHAPTER 4

THE REMOTE SENSING OF THE AQUATIC ENVIRONMENT

4.1. Remote Sensing of Intertidal Environments

Intertidal remote sensing differs from terrestrial and marine remote sensing in that the environment is periodically flooded due to tidal processes, and the physical and biological landscape is frequently and often substantially altered due to tides, storms (wind and wave action), currents, precipitation and desiccation. Consequently, the effects of these processes must be taken into account when examining the intertidal environment.

Although imagery for this research was acquired during low tide, the tidal level was not at its seasonal lowest, therefore certain vegetation and substrates in the lower littoral regions were submerged during imaging. As this study attempts to examine and classify the intertidal environment however, the boundary between intertidal and subtidal environments is not always clear, and not always recognized and paralleled by the distribution of intertidal organisms (Hruby 1976, Kozloff 1983). As a result, this study will need to address the problems of remote sensing vegetation and substrates that may be both submerged and emerged depending on the tidal level and spatial location on the beach.

In order to understand how a submerged region will differ spectrally from the same region in an emerged state, some knowledge of light interactions within the aquatic medium is required. The purpose of this section is to determine how the spectral signature of an object changes as it is submerged, and how its spectral properties are altered with increasing depth and varying amounts of dissolved organics, sediments and phytoplankton. To assist in the comprehension of the following section, some terms dealing with radiant energy and its interactions with matter are defined in Table 4.1.

Before a photon enters the aquatic medium, it must first pass through the air-water boundary known as the water surface. The amount of light that is reflected (or conversely,

Table 4.1. Definitions relating to the interactions with radiant energy and matter.

Definition	Description	Defined as
absorption	The process by which a molecule utilizes a photon. Absorption is often discussed in conjunction with a particular wavelength to illustrate the interactions between a certain wavelength and matter	
radiant flux	The time rate of flow of radiant energy. It is often expressed by Φ or F and given in watts (W).	Φ
radiance	The radiant flux per unit solid angle per unit projected area of a surface. Expressed as L and measured in watts per square metre per steradian. Radiance can also be written as $L(\theta,\phi)$ to indicate that L is a function of the zenith and azimuth angles.	$L(\theta,\phi) = d^2\Phi/dS \cos\theta \, d\omega$ where S is the cross sectional area of the surface point.
irradiance	The radiant flux incident on an element of a surface divided by the area of that element. Expressed using E and given in watts per square metre.	$E = d\Phi/dS$
reflectance	The ratio of the reflected radiant flux to the incident radiant flux.	$p = \Phi_r / \Phi_0$ where Φ_r is the reflected radiant flux.
transmittance	The ratio of the transmitted radiant flux to the incident radiant flux.	$T = \Phi_t / \Phi_0$ where Φ_t is the transmitted radiant flux
absorptance	The ratio of the radiant flux that is absorbed, to the incident flux.	$A = \Phi_a / \Phi_0$
scatterance	The ratio of the radiant flux scattered from a beam, to the incident flux.	$B = \Phi_b / \Phi_0$
absorption coefficient	The fraction of the incident flux that is absorbed divided by the thickness (Δl) of the layer.	$a = -\Delta A / \Delta l$ and expressed in metres -1
scattering coefficient *	The internal scattering within a layer divided by the thickness (Δl) of the layer.	$b = -\Delta B / \Delta l$ and expressed in metres -1
attenuance	The sum of the absorptance and scatterance, or the fraction of the incident flux lost to absorption and scattering.	$C = A + B$
attenuation coefficient	The total attenuance divided by the thickness (Δl) of layer.	$c = -\Delta C / \Delta l$ and expressed in metres -1

* Note: this scattering coefficient is also termed the total scattering coefficient, as the there is no directional attributes to the term. Other scattering coefficients include the forward, backward and volume coefficients which will not be used in this discussion.

Sources; Dera 1992, Kirk 1983, Williams 1970.

transmitted) from the surface depends on four factors. The first is the roughness of the ocean surface. If the surface is smooth, then only the solar angle is important in determining reflectance. A rough surface results in increased surface area where the angle of incidence at any particular location changes continuously, therefore the amount of reflected light also changes over time. Previous studies have found that imaging at high solar angles negates most of the effects of surface roughness with an average reflectance from smooth surfaces near 6.6% for cloudless days, and 5.2% for overcast days (Dera 1992, Kirk 1983, Williams 1970) .

The second factor affecting reflectance from a water surface is the solar angle (sun angle from the vertical). The greater the solar angle the greater the reflectance as seen from Table 4.2. Reflectance does not vary significantly under a sun angle of greater than 60° (Williams 1970).

Related to the effects of the solar angle on surface reflectance, is the contribution of scattered skylight to the total irradiance at the sea surface. As scattered radiation may strike the surface at any angle, much of it may be reflected due to a low angle of incidence. Although it is beyond the scope of this discussion to determine the amount of scattered light that reaches the surface at varying angles, the contribution of scattered skylight to the total radiant flux is given in Table 4.3.

The last factor contributing to surface reflectance is light that has penetrated the surface and has been re-emitted from the water column. This is the most difficult of the four processes to quantify, as many factors contribute to the underwater light field.

Table 4.2. Reflectance from smooth water at various solar angles.

Solar Angle	Reflectance	Solar Angle	Reflectance
0°	2.0%	50°	3.5%
10°	2.0%	60°	5.9%
20°	2.0%	70°	13.2%
30°	2.1%	80°	34.7%
40°	2.4%	90°	100.0%

(after Williams 1970)

Table 4.3. Percentage of scattered sky radiation to total radiation for a cloudless day.

	Solar Angle			
	50°	60°	70°	80°
Summer	27	32	42	67
Winter	15	20	28	59

(after Williams 1970).

The constituents contributing to the spectral properties of seawater are a) the water itself, b) Dissolved Organic Matter (DOM), c) inorganic matter, d) phytoplankton (Dera 1992, Tassan 1983).

4.1.1. *Water*

Water appears clear in small quantities but takes on its characteristic blue colour when present in large masses such as a lake or ocean. Many studies have measured the absorption coefficient of different water bodies, including distilled water, but the results of these studies are often inconsistent when measuring the same liquid (ie. distilled water). Absorption for pure water is given in Figure 4.1. Notice how absorption rise sconsiderably from @ 440 nm (blue) to the near infared, especially beyond the 550 nm region. Therefore, the blue regions of the spectrum exhibit the smallest rate of attenuation, and as a result are subject to the greatest scattering, which gives water its characteristic blue colour (Dera 1992, Kirk 1983).

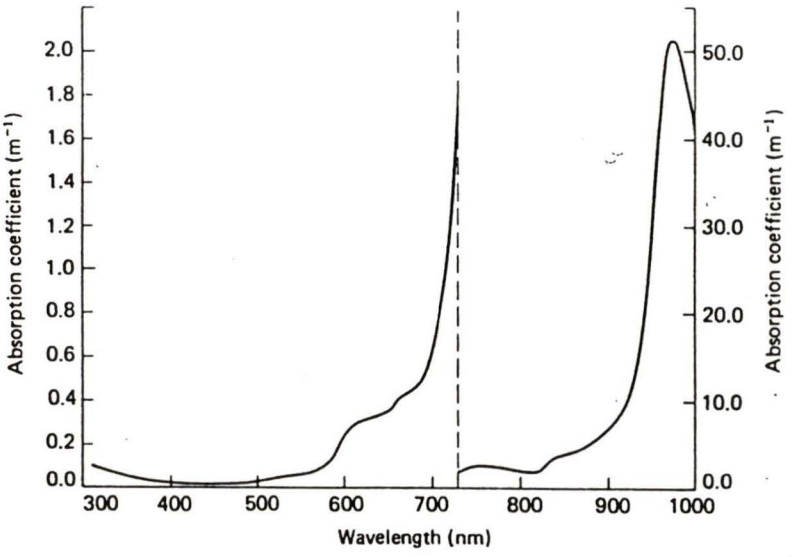

Figure 4.1. The absorption spectra of distilled water from 310 - 790 nm, and 790 - 1000 nm (after Kirk 1983)

4.3.2. *Dissolved organics*

All water contains some matter created by the decomposition of organisms by other organisms or through natural decay processes. This decomposed matter is termed humic substances, yellow substances, gilvin or dissolved organic material (DOM). Dissolved organics are comprised of numerous organic molecules, which will eventually be broken down into inorganic nitrogen, sulphur, phosphorous and carbon dioxide. Although these substances comprise only a small part of the total amount of water, they strongly absorb in the ultra-violet and blue regions and therefore give water a yellowish colour, or a brown colour when large amounts of yellow substances are present (Figure 4.2) (Dera 1992, Kirk 1983, Sathyendranath *et al.* 1989, Tassan 1988, Williams 1970, Zibordi *et al.* 1990).

4.1.3. *Inorganic matter*

Inorganic suspended particles, or tripton are thought to cause considerable scattering in ocean water, but their effects on the spectral properties of water is difficult to quantify (Bhargava & Mariam 1990, 1991, Ritchie *et al.* 1976). Suspended sediment generally increases reflectance from water bodies, as well as increasing the attenuation coefficient. Bhargava & Mariam (1991) concluded that the addition of suspended sediments to a test water body increased reflectance fairly evenly across the 500 - 1000 nm regions. The study also found that reflectance increases with a decrease in particle size (Bhargava & Mariam 1991).

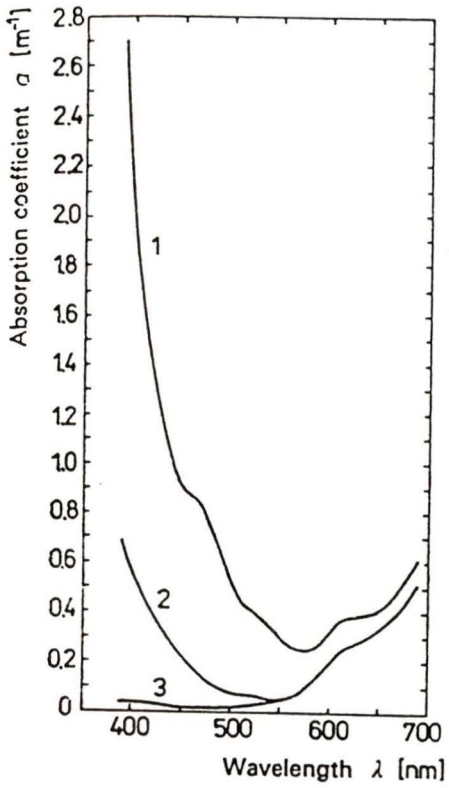

Figure 4.2. The absorption spectrum of clean water from the Sargasso Sea (3), compared with waters rich in dissolved organic matter from the Gotland Deep, Baltic Sea (2), and the Gulf of Riga, Baltic Sea (1)(Kopelevich & Burnkov 1977).

4.1.4. *Phytoplankton*

Phytoplankton are microscopic free floating photosynthetic organisms that constitute the primary trophic level of the marine food chain (Fogg & Thake 1987). Phytoplankton exist in all lakes and oceans where species, density and pigment composition can vary significantly over short distances. The organisms utilize the different forms of chlorophylls, carotenoids and biliproteins to harvest light, and therefore have a wide range of effects on the spectral reflectance of the water column. Phytoplankton generally gives lake and ocean water a greenish colour, as the chlorophylls are active in the blue and red regions of the spectrum. Certain species of phytoplankton, however, may turn water red or brown due to the carotenoid pigments in large blooms (red tides) (Stewart 1985). Spectral reflectances of waters containing different chlorophyll concentrations (phytoplankton) are given in Figure 4.3.

4.1.5. *Characterizing British Columbia's Coastal Waters*

The previous section discusses how the different constituents of water affect the total attenuation coefficient (c), and therefore the spectral reflectance of water. When remote sensing aquatic environments, it is useful to have some knowledge of the spectral properties of the water, especially if the objective of the research is to examine submerged features. Two species of intertidal algae located adjacent to one another, for instance, may have significantly different spectral signatures if one alga is submerged. Consequently, if some knowledge is available as to the spectral properties of the coastal waters, then there is some idea at which depth the spectral signatures of benthic features become unrecognizable. The following discussion is not meant to ascertain, nor provide a

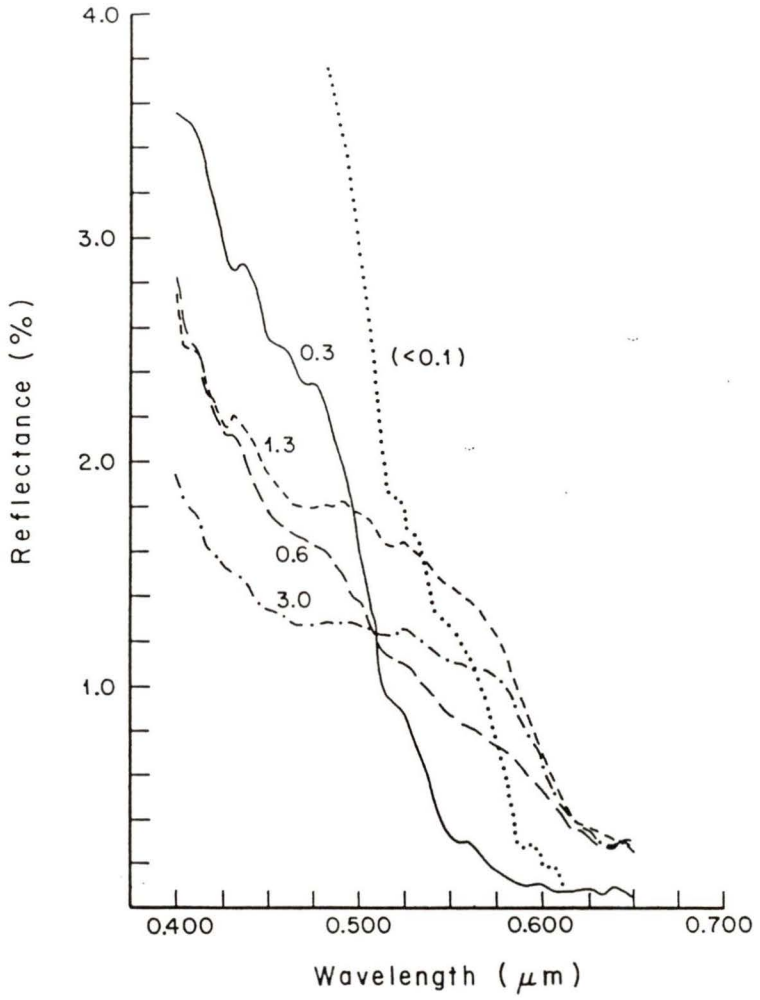

Figure 4.3. Spectral reflectance of seawater containing different concentrations of chlorophyll *a* over the NW Atlantic. Data were acquired from an aircraft at an altitude of 305 metres (Clarke *et al.* 1970).

detailed discussion of the optical qualities of British Columbia's waters, but to make the reader aware of some of the more general qualities of the coastal waters, and their possible effects on the spectral signatures of benthic features.

The coastal waters of British Columbia become extremely productive during the summer months, with chlorophyll *a* concentrations exceeding 40 mg per cubic metre during phytoplankton blooms (Gower *et al.* 1984). The average chlorophyll *a* concentrations for the waters surrounding Vancouver Island in July and August of 1979 were found to be 2.2 and 2.5 mg/m^3 respectively (Pan *et al.* 1988). The effects of different phytoplankton densities on ocean colour are plotted in Figure 4.3, and illustrate that chlorophyll *a* concentrations in the 2-3 mg/m^3 range significantly alter the vertical attenuation coefficient. Assuming the chlorophyll *a* concentrations were in this range (2-3 $mg/m^{3)}$ during imaging, it is possible that 50% of the incident flux passing through the air water boundary is attenuated per metre (light reflected from the benthos must again pass through the water column on its way back to the surface, effectively doubling the vertical attenuation coefficient). Chlorophyll *a* concentrations in the vicinity of 2 mg/m^3 would also result in poor water penetration in the blue regions, while the green wavelengths would reach furthest into the water column (see Chapter 2).

CHAPTER 5

METHODOLOGY AND DATA COLLECTION

5.1. Selection of the Bandset

The number, width, and placement of bands within the visible and near infared (NIR) spectrum is user configurable for the Compact Airborne Spectrographic Imager (CASI). Therefore, a bandset can be created that is suited for coastal applications. Ideally, the more bands used, the greater the spectral resolution, but as the collection of data is limited by the time needed to read the CASI's array and write to magnetic media, spatial bands are generally limited to less than 15. As the number of bands used increases (increased spectral resolution), pixels will become larger (decreased spatial resolution). The parameter that delineates this trade-off between spectral and spatial resolution is termed the integration time, which is the time needed to sample and record at each band. The integration time per band remains constant, therefore the higher the number of bands the greater the integration time and the lower the spatial resolution (Borstad & Hill 1989).

The first consideration in the creation of an intertidal bandset was to assess the importance of spatial resolution (pixel size) and determine an adequate resolution. The algae (seaweeds) and sea grasses of the coastal environment display a high spatial variability, as competition for space is intense, and the rapidly changing environmental conditions from subtidal to supertidal zones favors certain organisms at certain levels in the intertidal zone (Carefoot 1983, Dayton 1975, Druehl & Green 1982, Hruby 1976). As discussed in Chapter 3, the zonation of littoral environments is a result of the varying responses of marine organisms to environmental factors that are related to the tidal cycle. To adequately image different intertidal regions (including rocky coastlines) that exhibit a narrow zonation, a high spatial resolution is needed. As a result, the target pixel size was

set at two square metres (Carefoot 1983, Dayton 1975, Druehl & Green 1982, Hruby 1976).

The second consideration in choosing the bandset was to determine the number, width and placement of the spectral regions for examining intertidal vegetation. As previously discussed in Chapter 3, the spectral characteristics of seaweeds vary depending on the arrangement of the organisms' photosynthetic cells, the antecedent light conditions, and the effects of desiccation. For these reasons, bandwidths were selected that permitted a wide latitude in variations of the spectral properties of intertidal vegetation, rather than narrow regions specific to certain photochemical processes (ie. chlorophyll fluorescence) which may not be present throughout the intertidal region and have not traditionally been examined *in situ* in the littoral regions (Rowan 1989, Wiltens *et al.* 1978).

In designing the bandset, spatial resolution was given precedence over spectral resolution, and the number of spatial bands was limited to 8 in order to minimize pixel size. The spectral regions (bands) were selected for their ability to differentiate between intertidal vegetation, and chosen using knowledge of algal pigmentation, structure, and conclusions from previous research (Abbott & Holenberg 1976, Bold & Wynne 1987, Glazer 1981, Kirk 1983, Lee 1989, Luning 1981, Ragan 1981, Ramus & Rosenberg 1980, Ramus 1981, Rowan 1989). The rationale for each band is illustrated in Table 5.1.

5.2. Fieldwork

Initially, fieldwork was to be accomplished using *in situ* transect sampling combined with the use of a portable video camera to record each site in detail. The transect method was to use large fluorescent markers on the shore that could be seen on the image. These markers were to provide reference points that could be used to align data from the

Table 5.1. Spectral regions selected for use in an intertidal bandset.

Wavelengths (nm)		Uses of the spectral region
Band 1	431.6 - 459.4	Chlorophyll and carotenoid absorption. Clear water penetration.
Band 2	480.3 - 499.6	Discrimination between chlorophylls *a* and *b*. Clear water penetration.
Band 3	545.3 - 559.4	Identification of Phaeophytes (brown algae) due to carotenoid absorption. Penetration of organic and sediment rich water.
Band 4	601.8 - 614.2	Identification of Rhodophytes (red algae) due to biliprotein absorption.
Band 5	646.2 - 660.4	Chlorophyll *b* absorption.
Band 6	665.8 - 678.2	Chlorophyll *a* absorption.
Band 7	746.1 - 749.7	Detection of vegetation and biomass estimation.
Band 8	871.4 - 878.6	Detection of vegetation, biomass estimation and substrate identification.

Sources: Austin & Adams 1978, Bartlett & Klemas 1981, Bold & Wynne 1987, Glazer 1981, Kirk 1983, Lee 1989, Luning 1981, Ragan 1981, Ramus & Rosenberg 1980, Ramus 1981, Rowan 1989, Specht *et al.* 1973.

transects to the image. Using these markers as reference points, transects would run from the head of the shore toward the water at predetermined intervals along the beach. As the transect crossed a boundary between different substrates and/or vegetation, the distance from the head of the beach would be recorded. If transects were spaced 2-3 m apart (the size of an image pixel) and changes in surface cover along each one noted and recorded, a surface cover map could be produced which could then be compared to the classified imagery to determine classification accuracies.

Several problems, however, were encountered when testing the transect method, which rendered it inappropriate for this study. Problems with this technique are not inherent to the method, but the application of this technique to this study. As the shore must be sampled at low tide, where the low tide window rarely lasts over 2 hours, it would require many people to simultaneously set up and record transects at several locations. It is often not feasible or advisable to sample using transects on days prior to or after imaging, as low tide may occur at a different time, making sampling impossible, or the beach may be altered by tidal or wave action on previous or subsequent days. One method that could be used to reduce the amount of labour needed to sample all areas would be to concentrate sampling efforts on one or two sites that are deemed representative of several other sites. This solution, however, may be unacceptable if the sensor is not equipped with a roll correction mechanism. If the aircraft encounters turbulence over the sites that have been sampled, the imagery may be distorted and consequently the fieldwork does not correspond to the imagery. Therefore, it is possible that the only usable imagery may have been acquired from sites that were not sampled using the transects. This problem is exacerbated by the nature of coastal remote sensing. Unlike imaging a large scale object(s) such as a forest, where the aircraft has a large area in which to find calm, clear air, intertidal environments are very narrow regions. The aerial remote sensing of shorelines is also hindered by convection currents at the land/water juncture which result in platform movement due to turbulent air.

The use of transects also presented a problem in that markers left unattended were often removed by visitors to the study area, although the markers stated that their purpose was benign. Markers also tended to fade in the summer sun, which resulted in signs that were difficult to distinguish at a distance.

Due to the problems experienced with transects, the video camera was used in conjunction with samples identified in the laboratory. The use of a hand-held video camera allowed sites to be quickly filmed with great detail, and permitted five or six sites to be visited during the low tide window by one person, as contrasted with one or two sites ground truthed using transects and several people. The technique used in acquiring the video imagery was to walk along the beach parallel to the water and film from left to right, and then face backwards and also film from left to right. This method permitted permanent features on the shoreline (i.e. houses) to be used as reference points, which could later be referenced to the imagery. The main disadvantage to this technique is that positional information is not as precise as it would be if a transect method was used.

Samples of vegetation and substrate were collected while filming, where the location of the collected sample was filmed and recorded. Locations of sample sites are given in Appendix A.

5.3. Acquisition of Imagery

5.3.1. *Site Selection*

The selection of test sites for this study were subject to several criteria. First, the areas must be close to an airport so as to minimize aircraft rental costs. Therefore, only sites that were within 20 km of the airport were considered. Second, the regions to be imaged must be easily accessible for ease of fieldwork. Lastly, the sites chosen to be imaged should represent several different types of coastlines.

The Saanich Peninsula exhibits different types of shorelines, which include rock, cobble, sand and mud substrates. The peninsula also exhibits significant differences in biological productivity between the west and east regions. The eastern side is subject to heavy, nutrient rich currents which contribute to the area's high biological productivity, while the western side receives much less nutrients and therefore has a decreased level of productivity. There is only one estuarine region, and no areas of heavy surf on the peninsula.

5.3.2. *Imaging*

Imagery was acquired using the Compact Airborne Spectrographic Imager at 1538 m (5000') over the Saanich Peninsula, Vancouver Island from 1030-1230 hours on July 28 1991 during a 0.7 m low tide at 1135 hours (Canada 1990) (Figure 5.1). All imagery was acquired during a single flight. An attitude correction system was not yet operational on the Borstad Associates Ltd. CASI during imaging, therefore the resulting effects of aircraft roll can be seen in some of the imagery. Several study sites were flown, comprising examples of rock, sand, and mud substrates with a variety of vegetation on each site.

The two images chosen for this study were selected as they are a) free from roll errors, and b) exhibit examples of rock, cobble, sand and mud substrates which are host to many species of intertidal algae and one species of intertidal plant (*Zostera marina* or eelgrass) (Scagel 1967). The first image was acquired over Roberts Bay and Sidney Shore, and the second image over Island View Beach (Figures 5.2 - 5.3).

The advantage of using an imaging spectrometer over a more traditional multispectral scanner became apparent during imaging. Certain imaging spectrometers such as the CASI allow the operator to view reflected radiance in real time, or "on the fly" (Borstad & Hill 1989). As a result, changes can be made to the bandset during imaging to avoid saturated bands or bands with low contrasts. Band 1 was initially to be narrower

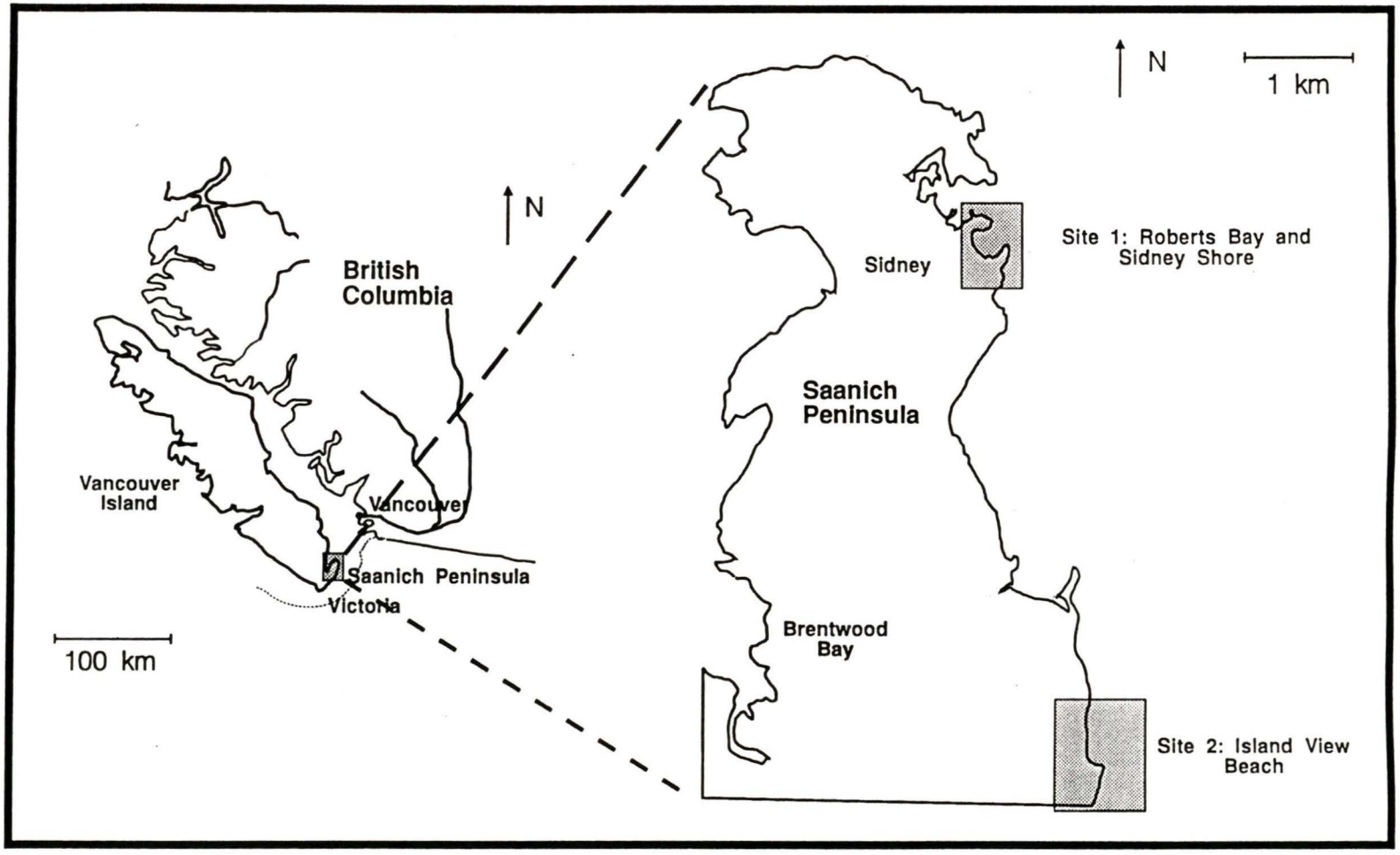

Figure 5.1. A map of southwestern British Columbia and the Saanich Peninsula illustrating the study sites used in this research.

Figures 5.2 and 5.3. Near true colour composites using bands 6, 3 and 1 for Roberts Bay, Sidney Shore and Island View Beach. Image size is 512 lines by 512 pixels, but has been stretched to 1024 lines to reflect the 2:1 aspect ratio of the pixels at the altitude at which the data were acquired.

than 27 nm, but low reflected radiance at these wavelengths required that the band become broader (Table 5.1). The two near infared (NIR) bands (7 and 8) were originally intended to be broader, but saturation at these wavelengths resulted in decreased bandwidths (Borstad & Hill 1989).

5.4. Site Description

5.4.1. *Sidney Shore and Roberts Bay*

Roberts Bay is composed predominantly of mud substrates with sand and gravel areas occurring towards the head of the beach. A small freshwater stream lined with pebbles and sand flows into the middle of the bay. Rock outcrops are present toward the edges of the bay. The waters within the bay are generally very shallow (< 2 m) at low tide and brackish, where submerged benthic features appear differently to the naked eye than similar emerged features at approximately 1 m depth. The bay is very calm, with minimal wave and current action, even on windy days (Figures 5.4 - 5.5).

Blidingia spp . Kjellman, *Enteromorpha spp.*, and *Ulva spp.* are the predominant algal genera found on the mud substrate. Sparse areas of *Pilayella spp.* are found attached to gravels and pebbles on the mud substrates, and generally found in conjunction with *Enteromorpha.* A single area of the Rhodophyte *Gracilaria verrucosa* Hudson is also present, but almost completely buried in mud substrates and often covered by the Chlorophytes. Vegetated areas in the lower intertidal zone often contained a mixture of species with certain areas supporting sparse patches of the sea grass *Zostera marina. Fucus distichus* is the dominant algae found on the rocky areas in the bay. The supra littoral fringe (head of the shore) near the middle of the bay contained a large area of terrestrial grass interspersed with shallow (< 1 m) oligotrophic

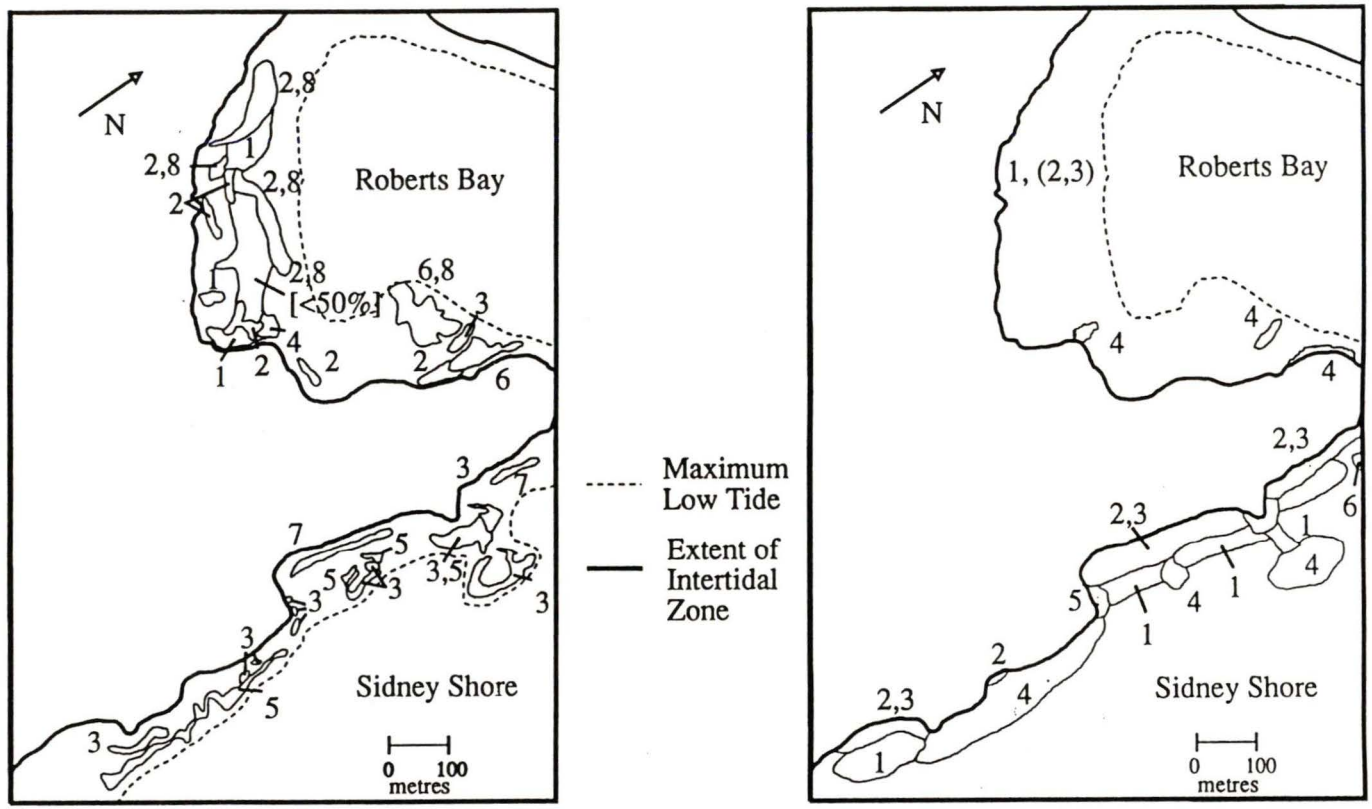

Figure 5.4 and 5.5. Intertidal vegetation and substrates of Roberts Bay and Sidney Shore. Data were acquired using a portable video camera and the collection of samples for later identification in the lab. The terrestrial/marine boundary was digitized from the CASI imagery.

pools of water with sand and gravel bottoms. At low tide, exposed vegetation in the mid to lower intertidal regions remained wet, while the vegetation of the upper intertidal regions had undergone desiccation (Scagel 1967).

The shoreline north of the Sidney breakwater (Sidney Shore) is composed mainly of rock outcroppings surrounded by sand and gravel areas. *Fucus distichus* covers rocky areas in the higher intertidal zone while *Monostroma spp.* occupies the zone beneath the *Fucus*. A layer of Chlorophyte detritus approximately 1 m in width is found near the head of the beach. Large non-vegetated areas composed of sands and clays are found in the middle and lower intertidal zones, and certain areas of the rocks are covered with dense accumulations of shell fragments.

5.4.2. *Island View Beach*

The shoreline of Island View Beach is composed mainly of sands, gravels, and cobbles, and has large submerged offshore bars composed of eroded sand and clay from cliffs bordering the ocean (Figures 5.5 - 5.6). Vegetation in the region is limited to intertidal areas of *Monostroma spp.* and subtidal *Nereocysits* (bull kelp) beds. Absolute amounts of biomass on Island View Beach is less than Sidney Shore, and much less than Roberts Bay. Large amounts of suspended particles combined with a high biological productivity resulted in water where the appearance of submerged vegetation and substrates at a 1 metre depth was significantly different than their corresponding exposed features.

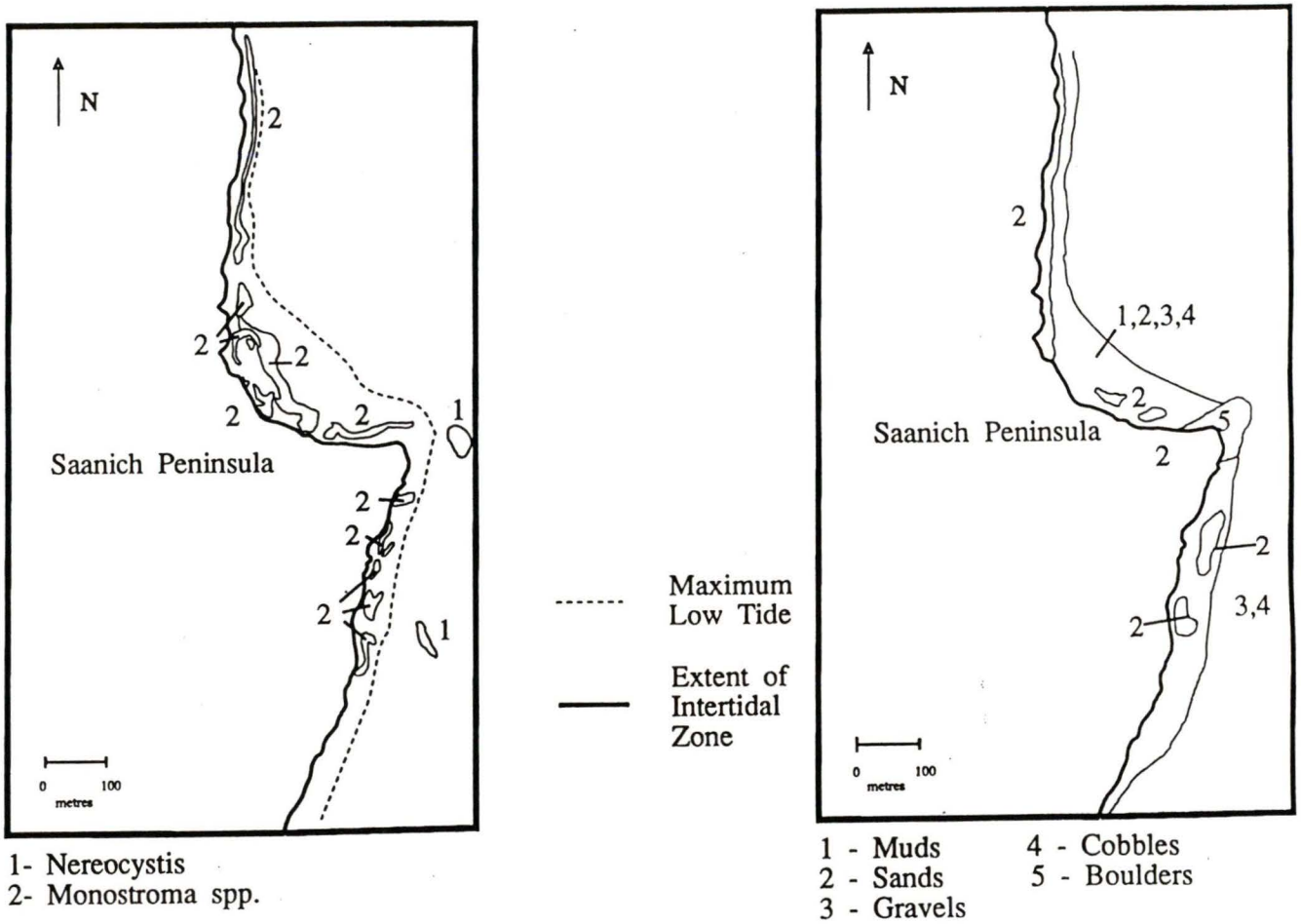

Figures 5.6 and 5.7. Intertidal vegetation and substrates of Island View Beach. Data were acquired using a portable video camera and the collection of samples for later identification in the lab. The terrestrial/marine boundary was digitized from the CASI imagery.

CHAPTER 6

ANALYSIS OF THE IMAGERY

6.1. Spectral Properties of Intertidal Vegetation

6.1.1. *Introduction*

Radiance plots of intertidal vegetation were examined and compared to spectral signatures derived from other theoretical and applied studies. Radiance plots were acquired by locating the line and pixel addresses of homogeneous areas of vegetation, and the radiance values of these areas written to a file for each of the eight bands. The intertidal region is composed of hundreds of spectrally unique components, therefore the 2.5 m resolution of the CASI limited the generation of signatures to larger areas. For this study, only areas greater than 5x5 pixel regions were used, as smaller areas could not be accurately located using the video camera. Standard deviations for the radiances have been included to give some indication as to the homogeneity of the sample sites, and the effects of moisture on intertidal signatures.

A problem that is of importance when examining spectral signatures of the intertidal environment is that of substrates obscuring vegetation. As most intertidal vegetation has a small vertical component and tends to grow parallel to its habitat rather than vertically, substrates can easily be washed onto the vegetation by tides and waves, which may alter their spectral signature. Littoral species with a large vertical component, such as certain sea grasses may also be bent towards the surface due to mud or dead vegetation clinging to the stalks. These flattened grasses and algae can appear differently on imagery than grasses in their normal vertical state.

The presence of mud on vegetation may be detected by a higher than normal red reflectance (Budd & Milton 1982). The presence of dead vegetation (detritus) within the

algal (or sea grass) canopy may also alter the spectral properties of the live species, although detritus can be identified by its low NIR reflectance and increased red and middle IR reflectance (Budd & Milton 1982, Hardisky *et al.* 1984).

6.1.2. *The Chlorophytes (green algae)*

The reflected radiance of *Blidingia spp.*, *Enteromorpha spp.* and *Monostroma spp.* is plotted in Figure 6.1. The reflectance properties of these genera in the 400-700 nm regions are typical of most terrestrial and marine organisms utilizing the chlorophylls as the primary photosynthetic pigments. The three genera have similar spectral responses in band 1, characterized by low reflectance due to the presence of the chlorophylls and certain carotenoid pigments (Bold & Wynne 1978, Kirk 1983, Lee 1989, Rowan 1989). Towards the green region of band 3, reflectance increases as green light is only minimally used by the chlorophylls. *Blidingia* beds are bright green and therefore exhibit a greater reflectance. Reflectance in bands 4, 5 and 6 declines toward the red end chlorophyll absorption regions in band 6 (Rowan 1989).

Above 700 nm, terrestrial photosynthesizing plants reflect almost all of the near infared (NIR) radiation received (Avery & Berlin 1992). The mechanisms behind this phenomena are not fully understood, but it is thought to be due to discontinuities in the refractive index caused by the air-cell wall interface (Gates *et al.* 1965, Lee 1989). Marine algae also exhibit high NIR signatures, although the mechanisms contributing to this phenomena may be somewhat different for certain Phaeophytes (Lee 1989, Rowan 1989). The NIR regions have been successfully used in the detection and differentiation of terrestrial vegetation, but these wavelengths become less useful in the intertidal environment due to the presence of water.

The differences in reflected radiation for the three genera are quite varied in the NIR regions (Figure 6.1), but the differences are often a result of the presence of moisture rather

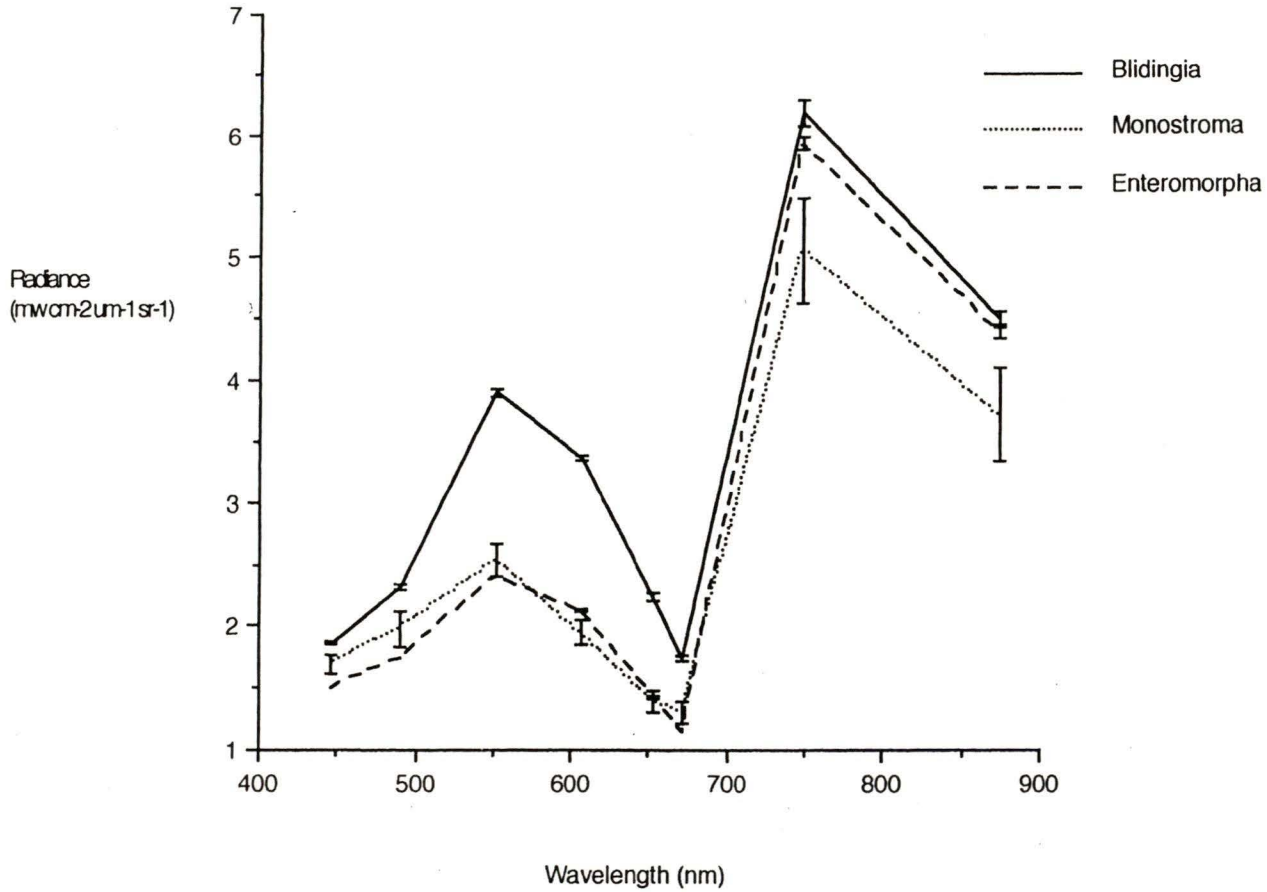

Figure 6.1. Radiance plots of *Blidingia spp.*, *Monostroma spp.* and *Enteromorpha spp.* Error bars represent the standard deviation for each sample.

than differences in the organism's spectral properties, as water is a strong absorber of the IR wavelengths (Avery & Berlin 1992). As a result, the IR spectral signatures of intertidal seaweeds are dictated by both the spectral properties (pigmentation and algal structure) of the organism and its water content, or state of submersion (Bartlett & Klemas 1981, Budd & Milton 1982, Gross *et al.* 1986, Jensen & Lorenzen 1988, Kirk 1983). As there are large variations in the moisture content of the intertidal zone which change with tides, precipitation, evaporation, desiccation, storms and wave action, the IR signatures for the intertidal region may have little to do with the spectral properties of the algae (McConnaughey & McConnaughey 1986).

The effects of moisture on NIR vegetation signatures can be demonstrated using Chlorophyte beds which are either immersed or exposed. Areas of exposed and submerged mixed Chlorophytes are plotted in Figure 6.2, where the spectral signatures of the algae diverge in the NIR, and the standard deviations increase. The high standard deviations are most likely due to different water/algae ratios within the communities. Similar results for algae mapping in the Venice Lagoon were found by Zibordi *et al.* (1990).

6.1.3. *The Phaeophytes (brown algae)*

Only three Phaeophytes were present in significant quantities for homogeneous areas to be imaged using the CASI. *Fucus distichus* was present at Roberts Bay and Sidney Shore and *Nereocystis* beds were present at Island View Beach. Although *Nereocystis* is a subtidal kelp, it will be included in this discussion as is occurs in near shore zones. The third brown algae, *Pilayella spp.* is sparsely distributed over large areas of Roberts Bay, and is often found in conjunction with *Enteromorpha* (Carefoot 1983, Scagel 1967).

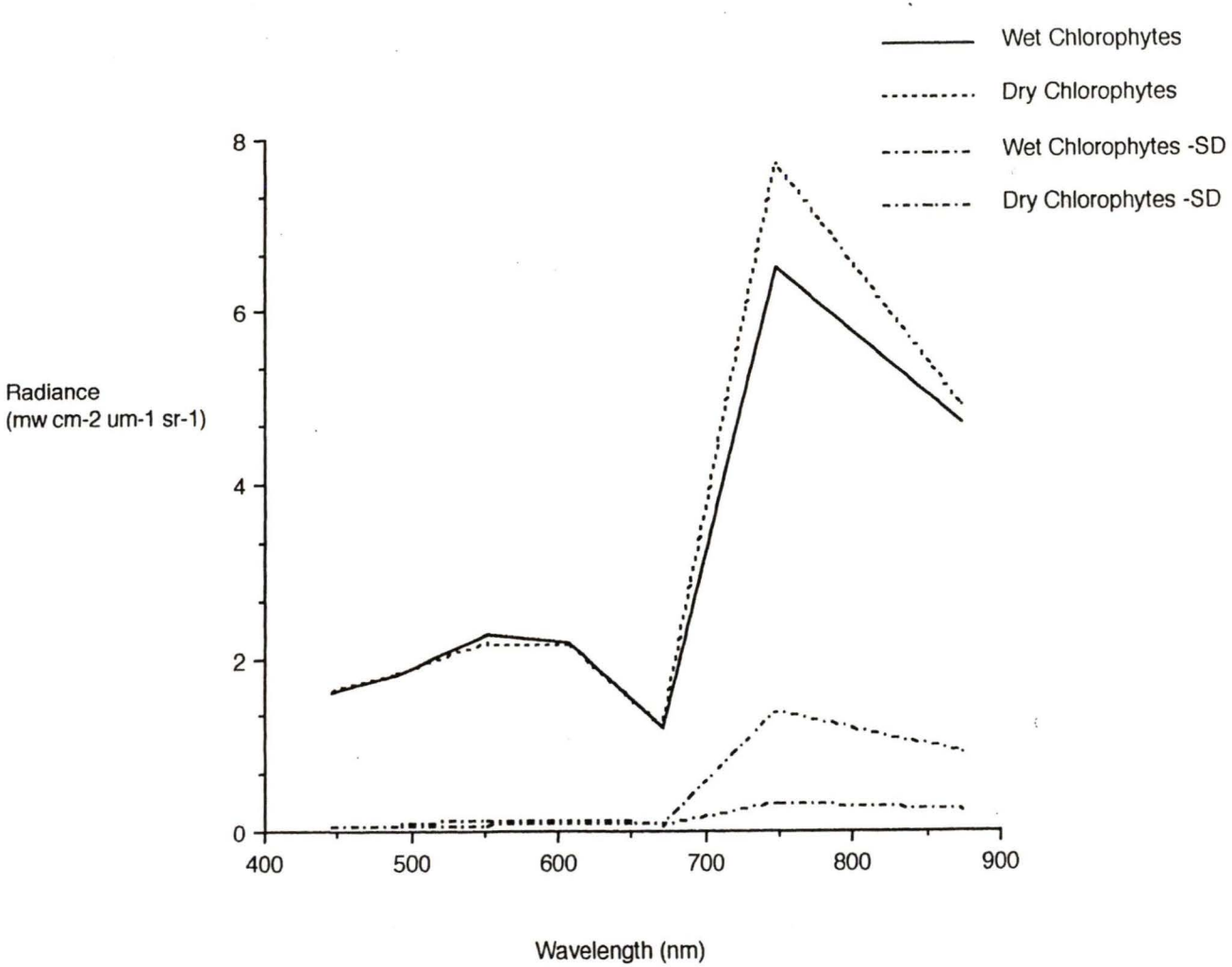

Figure 6.2. Radiance plots of wet and dry mixed Chlorophyte communities containing *Ulva spp.*, *Enteromorpha spp.*, *Monostroma spp.* and *Zostera marina.* Standard deviations for each community are also plotted as lines rather than error bars to facilitate legibility.

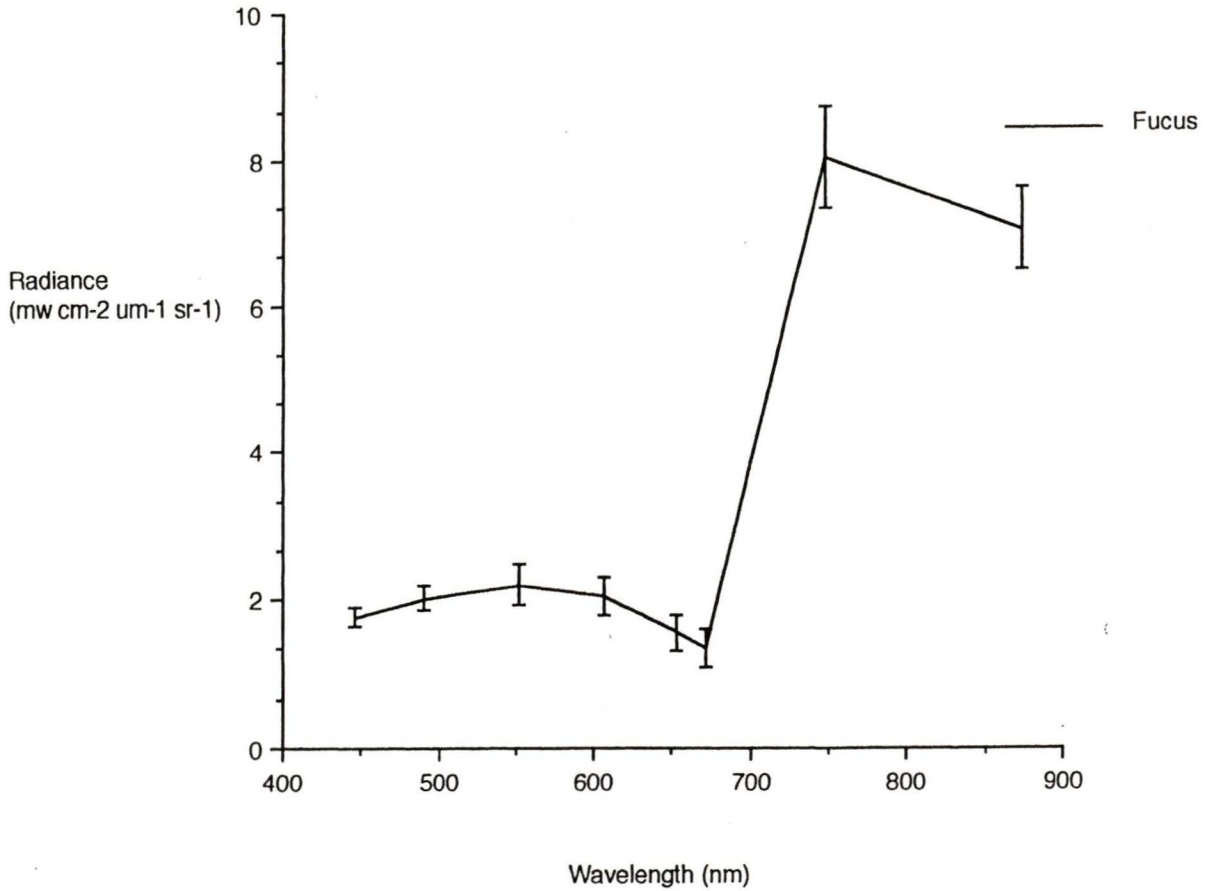

Figure 6.3. A radiance plot of *Fucus distichus* (a Phaeophyte). Error bars represent the standard deviation of the sample.

Radiance plots of *Fucus distichus* are shown in Figure 6.3. As *Fucus* uses both chlorophylls and carotenoids to harvest light, its spectral signature in the green regions is distinctly flatter when compared with the Chlorophytes. This is due to the utilization of light in this region by the carotenoids, mainly fucoxanthrin and *B* - carotene (Rowan 1989). As with the Chlorophytes, the NIR reflectance standard deviations are both high, which may indicate fluctuating amounts of moisture (Figure 6.3).

The radiance plot of *Nereocystis* is shown in Figure 6.4. As the cumulative reflectance from the bed includes the water between kelp fronds and bulbs, the spectral characteristics of clear water adjacent to the bed are also plotted on Figure 6.4. From the plots it can be seen that the NIR regions are probably best suited for differentiating floating kelps from water, which supports previous research in this area (Augenstein *et al.* 1991, Jamison 1972, Jensen *et al.* 1980). Bands 2 and 3 also show decreased reflectance from the beds, which is most likely due to the harvesting of light by chlorophylls and carotenoids (Rowan 1989).

From the radiance plots shown above, the optimum spectral region for discriminating between Chlorophytes and Phaeophytes would seem to be band 3 (green) as the absolute differences between the classes is greatest in the 550 nm regions. Difficulties in identifying intertidal vegetation may occur when using the NIR wavelengths, as the presence of water tends to alter the NIR signatures of the algae. Floating kelps are probably best identified using the NIR regions, and possibly the blue and blue-green wavelengths as well.

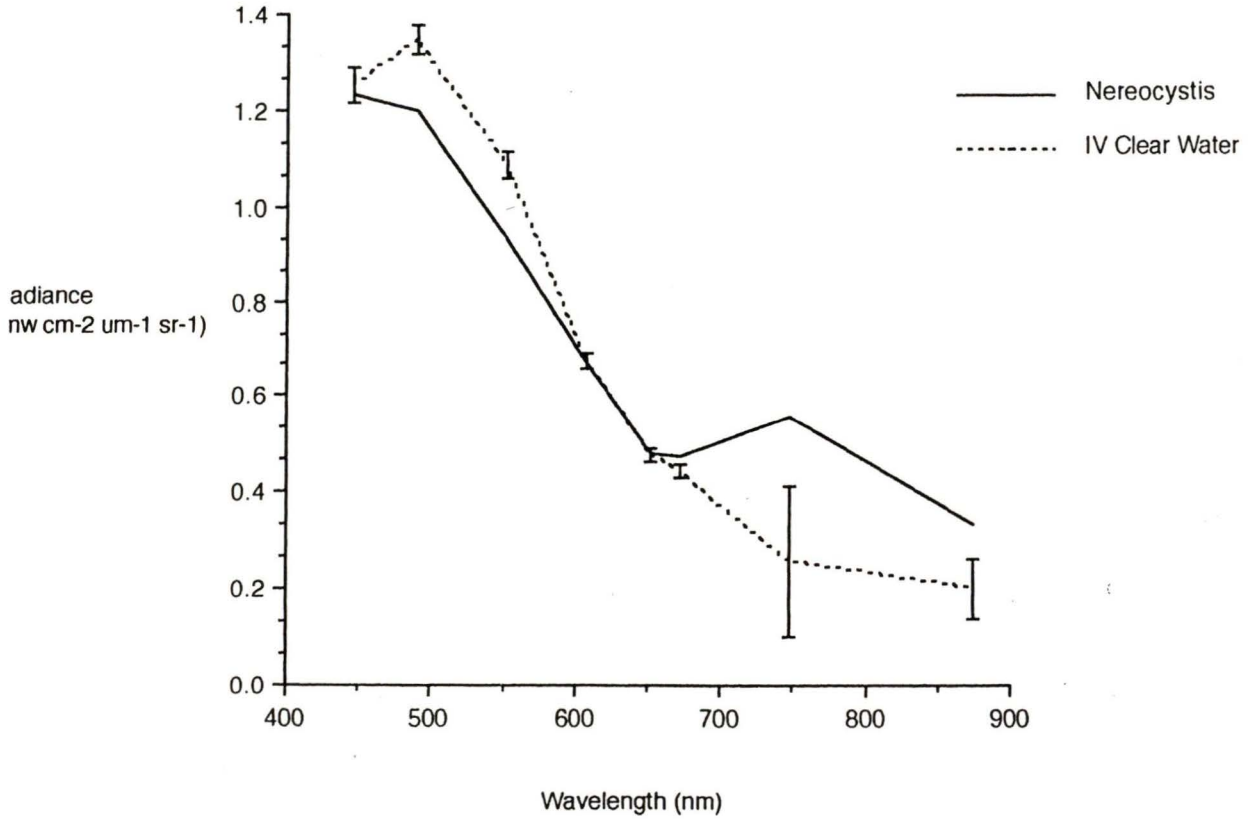

Figure 6.4. A radiance plot of a *Nereocystis* bed at low tide and the kelp free water adjacent to the bed. The greatest spectral difference between the kelp and the water is evident in band 7. Error bars represent the standard deviation for each sample.

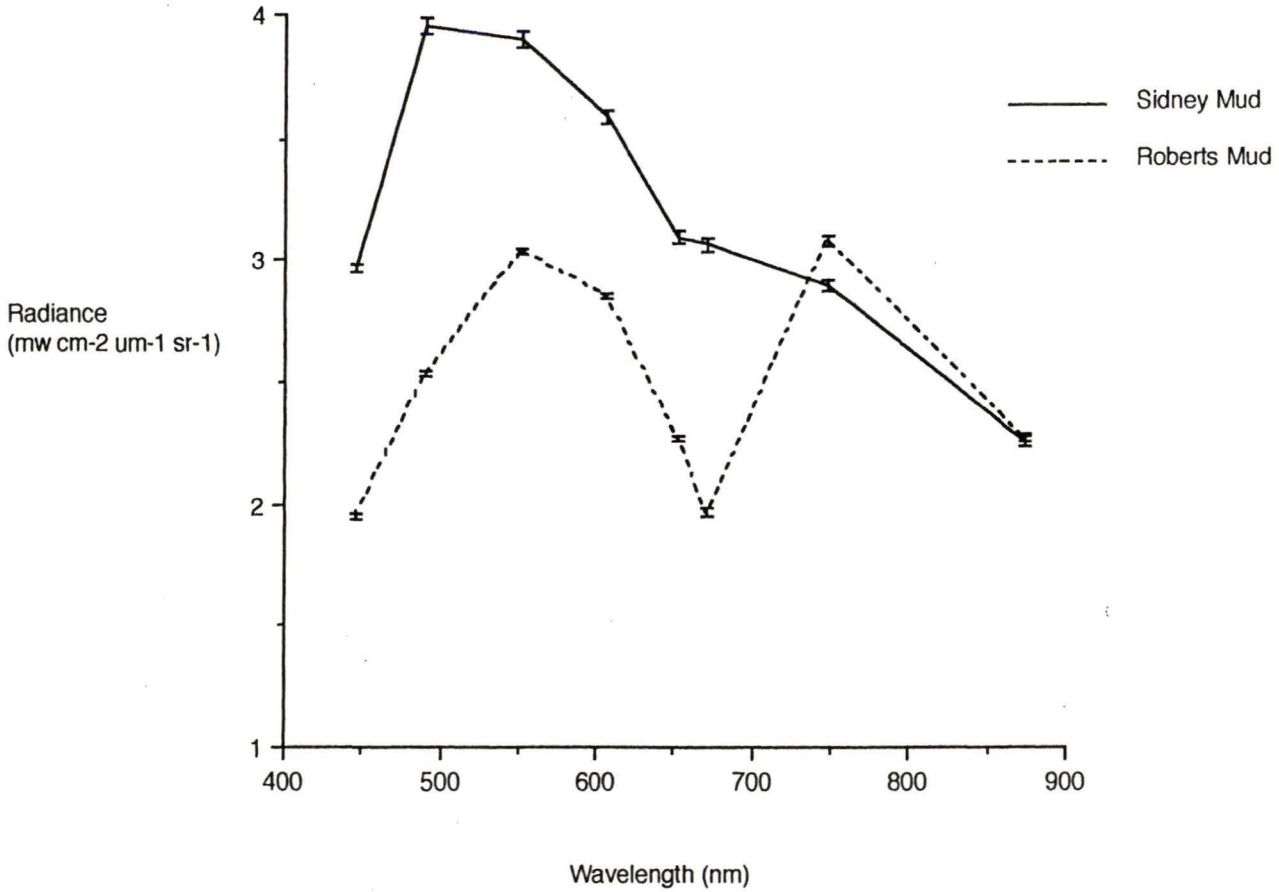

Figure 6.5. Radiance plots of clay/silt substrates from Roberts Bay and Sidney Shore. Error bars represent the standard deviation for each sample.

6.2. Spectral Properties of Intertidal Substrates

Several types of substrates occurred in homogeneous patches that were sufficiently large to be identified on the images. The fine grained substrates (Figure 6.5 included the clays and silts of Roberts Bay and Sidney Shore, where Roberts Bay contained greater amounts of organics and detritus than the relatively inorganic clay/silts of Sidney Shore .

Radiance plots of Roberts Bay mud substrates resemble the spectral properties of vegetation, which illustrates the effects of vegetation and/or detritus on substrate reflectance. The most noticeable differences in the two substrates are in the chlorophyll *a* absorption regions of bands 5 and 6, and the NIR regions of band 7. Sediments containing vegetation are the most difficult to discern from inorganic materials in the blue regions, although the chlorophylls are photosynthetically active in these regions. This may due to a) low blue reflectance of many materials, particularly in the near UV regions of band 1, and b) poor near UV performance of the CASI (G. Borstad, personal communication).

Radiance plots of sands for Roberts Bay and Island View Beach are shown in Figure 6.6. Reflectance for the Island View sands are similar to those of other intertidal substrates, but the signature of the Roberts Bay sands is unusual as radiance declines considerably in the green and yellow regions. The reasons for this decline are unknown, but may be due to changes in the bandset during image acquisition to avoid saturation, or a poor choice in sample sites. The later explanation is substantiated by a relatively large standard deviation for the Roberts Bay sands.

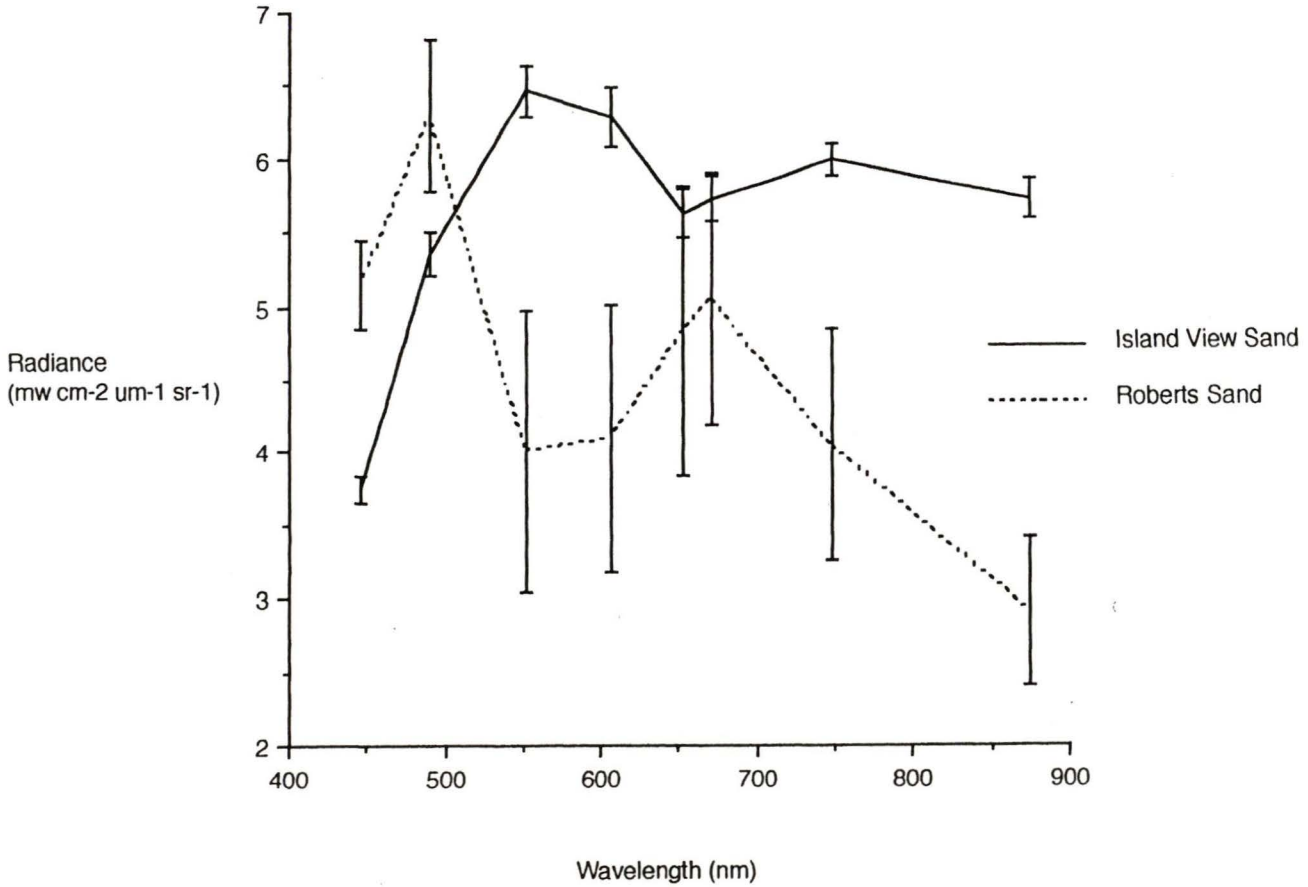

Figure 6.6. Radiance plots of sands from Island View Beach and Roberts Bay. Error bars represent the standard deviation for each sample.

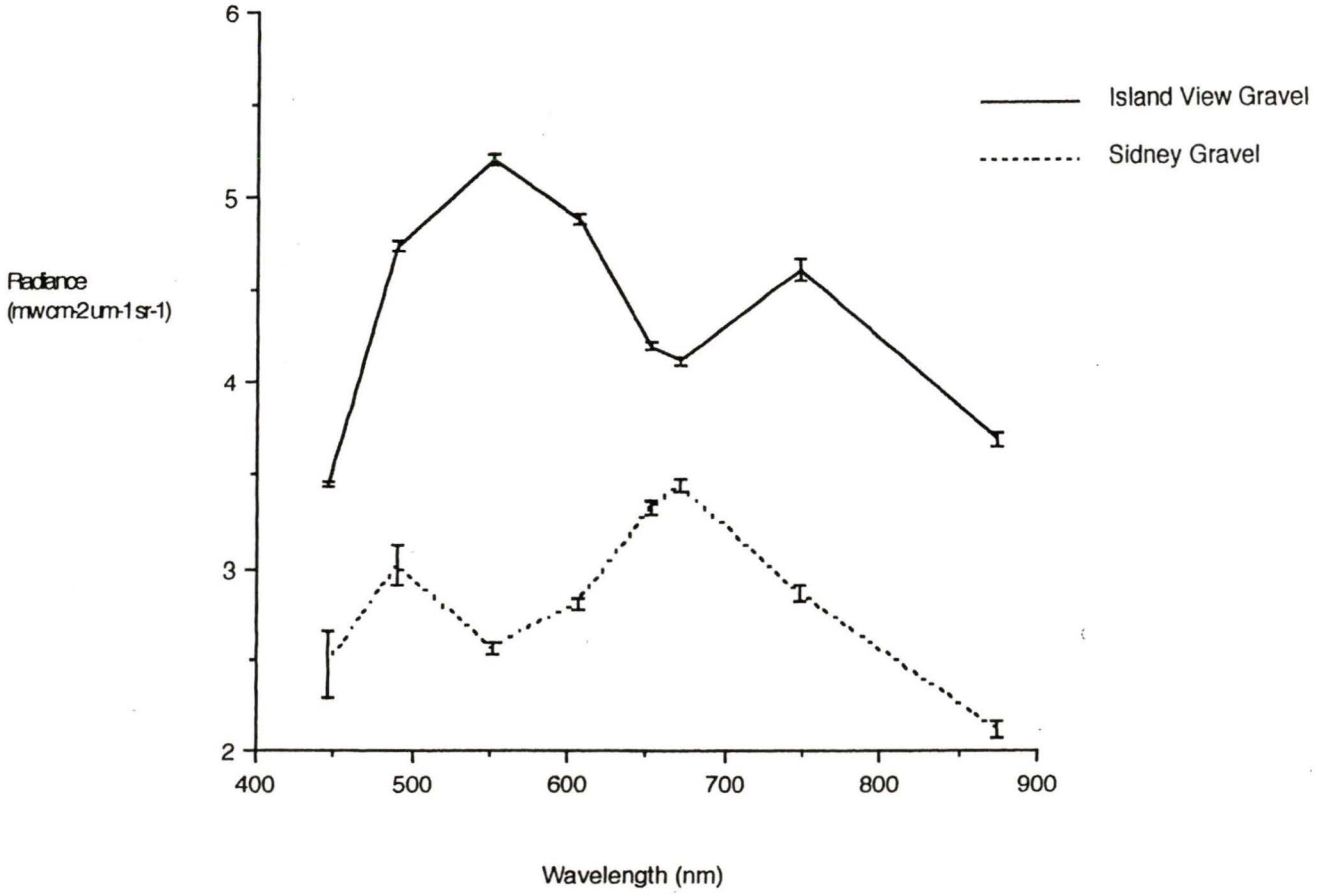

Figure 6.7. Radiance plots of gravel/cobble substrates at Sidney Shore and Island View Beach. Error bars represent the standard deviation for each sample.

No text on this page

Radiance plots for gravel/cobble areas in Roberts Bay and on Island View Beach are given in Figure 6.7. Signatures differ in bands 3 through 7, as the Island View materials exhibit vegetation like signatures. Again, this is probably due to vegetation occurring in conjunction with the substrates.

6.3. Interrelationships Between Bands

Between band correlation matrices for the intertidal and nearshore regions are given in Tables 6.1 - 6.2. The visible regions are highly intercorrelated, as are the two NIR bands - which is to be expected - but the degree of correlation is exceptionally high for within the visible and NIR bands as well as between the visible and NIR. Most terrestrial vegetation studies, and certain intertidal marshland research (Budd & Milton 1982, Hobbs & Shennan 1986) find that the visible and NIR regions often exhibit minimal or negative correlations as vegetation harvests light in the blue and red regions, while reflecting in the infared (Gates *et al.* 1965, Jensen & Lorenzen 1988). The most plausible explanation for the high degree of association found in this study is that the amount of biomass present in the two study sites is not sufficient to give the characteristic low or negative relationships found in terrestrial studies. Although vegetation covers much of Roberts Bay and Sidney Shore, the algal cover is often thin and partly covered with a layer of mud, and consequently the dominant spectral signatures of the region are those of the substrates. These findings were also reported to a lesser degree by certain other authors (Budd & Milton 1982, Donoghue & Shennan 1987, Gross *et al.* 1986, Hobbs & Shennan 1986, Tucker & Miller 1977).

The correlations for the Sidney image vary in a somewhat predictable manner according to knowledge of pigmentation and algal structure. As chlorophyll a is the dominant pigment for the vegetation, the green regions (band 3) are slightly more correlated with the NIR regions than other regions - with the exception of band 4 - as vegetation is

Table 6.1. Correlation matrix for intertidal/nearshore areas of the Sidney Image.

Bands	1	2	3	4	5	6	7	8
1	1.000							
2	.980	1.000						
3	.959	.966	1.000					
4	.950	.957	.980	1.000				
5	.963	.972	.980	.980	1.000			
6	.971	.979	.970	.972	.980	1.000		
7	.673	.655	.748	.754	.709	.669	1.000	
8	.686	.669	.746	.751	.716	.682	.980	1.000

Table 6.2. Correlation matrix for intertidal/nearshore areas of the Island View image

Bands	1	2	3	4	5	6	7	8
1	1.000							
2	.949	1.000						
3	.904	.937	1.000					
4	.901	.928	.975	1.000				
5	.897	.921	.957	.980	1.000			
6	.881	.908	.955	.978	.975	1.000		
7	.633	.639	.704	.743	.761	.777	1.000	
8	.722	.714	.754	.748	.721	.731	.950	1.000

reflective in both the green and NIR wavelengths. High band 4 correlations may be due to carotenoid absorption in the blue and green wavelengths or the spectral characteristics of the substrates. This trend was not as evident in the Island View scene, probably due to smaller amounts of vegetation present.

As most of the spectral reflectance in the two scenes can be attributed to substrates, between band correlations may not be the optimum method for assessing the information content of the bandset for vegetation mapping. The extremely high correlations between the bands in both the visible and NIR bands suggest that it may be possible to use one or two visible bands as a surrogate(s) for other visible bands, and only use one NIR region as both are also highly correlated. To test this hypothesis, a Principal Components Analysis (PCA) was employed to attempt to understand how each band contributes to vegetation and substrate identification.

6.4. Principal Components Analysis

6.4.1. *Introduction*

Principal Components Analysis (PCA) is a mathematical transformation that allows an insight into the interrelationships between several variables. The technique can be used to a) identify groups of intercorrelated variables, b) reduce the number of variables being studied, and c) manipulate a dataset into new variables (Johnson 1980). Any n by n correlated set of data - including multispectral bands - can be input into the analysis to achieve a transformed or uncorrelated n by n dataset. The PCA transformation is illustrated in Figure 6.8, where the pixel values of two bands are plotted against each other. The use of only two bands in the example is for illustration purposes, as the transformation can include n bands (variables), which would make the plot n dimensional. Figure 6.8

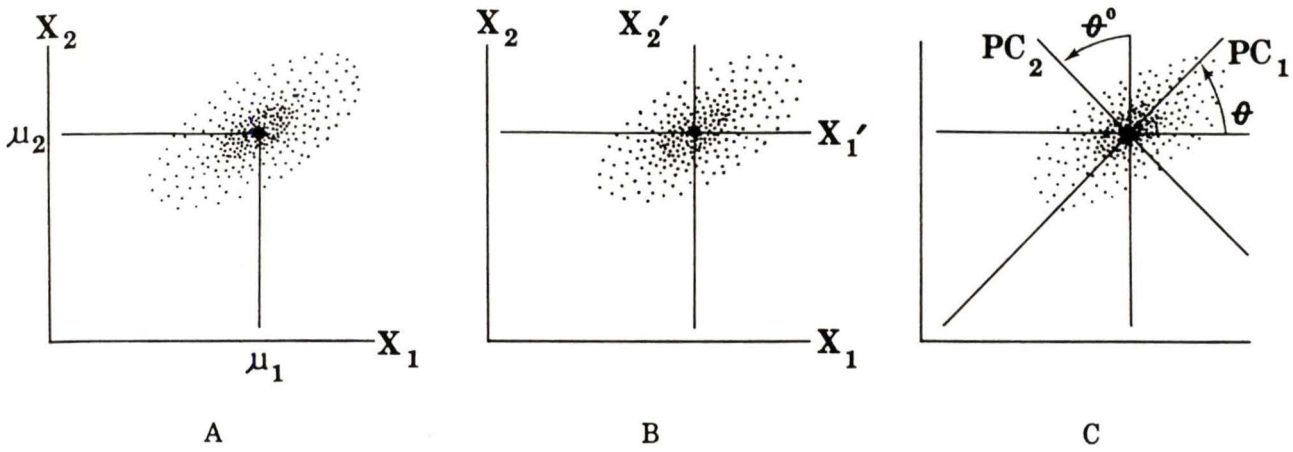

Figure 6.8. An illustration of two variables (bands) plotted against each other. In plot A, data points are clustered about the mean. A PCA redefines the axes where the mean becomes the 0,0 X and Y intercept (plot B). Data points are reassigned new values that correspond to the new axes. The axes are then rotated (plot C) until the variance of PC2 is at a maximum. The points that fall within the rotated area become PC1 and PC2 respectively (after Jensen 1986).

shows that the pixel values are clustered around the mean (small variance), which indicates that the bands are highly correlated with each other. Consequently, there will be difficulty in interpreting information from these bands due to a high degree of inter-correlation. If the axes of the plot however, could be rotated or translated to highlight the variation between the two bands, the information could be presented in a less correlated manner. This is accomplished by creating a new coordinate system (X_1' and X_2') where each pixel value is assigned new coordinates by $\mathbf{X_1' = X_1 - \mu_1}$ and $\mathbf{X_2' = X_2 - \mu_2}$ (Figure 6.8). The new axes (X_1' and X_2') become Principal Component 1 (PC1) and Principal Component 2 (PC2) respectively where the axes are rotated until the variance of PC2 is maximized. In this way the information in PC1 and PC2 is uncorrelated, and the two components generally account for greater than 90 percent of the scene variance (Jensen 1986, Johnson 1980, Richards 1986).

In the case of remote sensing, a PCA is often used to reduce an *n* channel dataset into fewer channels, where the information in the rewritten component channels is highly correlated within the component channel, and exhibits low correlations when contrasted to other components (Jensen 1986, Johnson 1980, Richards 1986). For this study, the PCA will be used to separate information pertaining to the identification of vegetation and substrates from spectral information that cannot be used to identify these features (Jensen 1986, Johnson 1980, Richards 1986).

Principal Components Analysis has been applied to the marine environment for deriving chlorophyll *a* concentrations from remotely sensed imagery, but there has been minimal research using PCA as a tool for examining intertidal imagery (Gower *et al.* 1984). One of the few applications of this technique to the intertidal environment was performed by Budd & Milton (1982), where a hand-held four channel radiometer was calibrated to the first four Thematic Mapper bands (blue, green, red, NIR) (Table 2.1) and used to examine an intertidal/saltmarsh area in southern England. The study generated four components (PC1 through PC4), where the first two accounted for 97% of the total image variance

(also termed the trace). PC1 was almost solely related to infared reflectance, while the second component represented much of the visible regions. The information content in PC1 was found to be unrelated to species type, whereas PC2 represented differences in canopy shadows and pigment absorption. PC3 was the only component that could be used for species discrimination, but accounted for only 2.06% of the trace. The study concluded that the IR wavelengths could not be used in species identification, but could be used in biomass estimation (Budd & Milton 1982).

Hobbs & Shennan (1986) also used a PCA on data gathered using a hand-held radiometer configured to the first four TM bands. The study attempted to discriminate between coastal marshland and non marshland using reflectance data from the radiometer. The data were clustered using several different classification techniques, as well as ordinated using a PCA, but the study found that the application of a PCA to clustered data did little to improve results. The use of the PCA in Hobbs & Shennan's (1986) study differs from the application to Budd & Milton (1982) and this research, in that raw data - as opposed to clustered data - is input into the PCA in this research and that of Budd & Milton (1982). Consequently, conclusions from the Hobbs & Shennan (1986) study on the use of the PCA for intertidal research may not be comparable to conclusions reached in this study, as the technique was applied to improve previously clustered results (Budd & Milton 1982, Hobbs & Shennan 1986).

Khan *et al.* (1992) used a PCA in the mapping of subtidal habitats in Saudi Arabia, but only used the first two TM bands in the analysis and used the technique solely for elimination of differences in reflectance due to depth. As a result, the use of a PCA in the Khan *et al.* (1992) study also has little bearing on the methods, results and conclusions of this research (Khan *et al.* 1992).

6.5. Application of a Principle Components Analysis

A PCA was performed on both the Sidney and Island View data sets. All eight input (raw) bands were entered into the analysis and eight new images, termed component images, or eigenchannels were generated. For each component, the eigenvectors (also termed component loadings) and squared eigenvectors for the component are given. Each eigenvector represents the product moment correlation coefficient between the component and the input variables (raw image bands in this case), while the squared eigenvectors represent the amount of variance in the component that can be attributed to an input variable (Tables 6.3 - 6.6). Tables 6.7 and 6.8 give the proportion of variance that each component (eigenchannel) contributes in relation to total image variance (Jensen 1986, Johnson 1980, Richards 1986).

Each component image was examined using subjective evaluations against all other components and comparisons with field data to determine the value of the component for identification of intertidal seaweeds, sea grasses and substrates. If the component image contained valuable information, the eigenvectors of that component were examined to determine the eigenvector loadings and squared eigenvector loadings on the input (original) bands. The purpose of this process is to derive a quantitative assessment of the value of the input spectral bands for discriminating between intertidal vegetation and substrates. As a result, the component images or the input bands that contain the most relevant information can then be used in the classification of the images, which decreases processing time and reduces the need for storage space (Jensen 1986, Johnston 1980, Richards 1986).

As there are data from two different types of coastlines (Sidney and Island View), the results from each scene can be compared to determine if the component loadings on bands for different littoral areas are similar. If there are similarities, then these bands may be useful to include in any subsequent intertidal studies.

Table 6.3. Eigenvectors of the covariance matrix from the Sidney image.

	Eigenvector (Component) Number							
Bandwidths (nanometers)	1	2	3	4	5	6	7	8
(1) 431.6 - 459.4	.151	.200	.409	.435	.404	.342	.347	.422
(2) 480.3 - 499.6	.112	.173	.223	.228	.283	.285	-.530	-.641
(3) 545.3 - 559.4	-.264	-.306	.407	.431	-.112	-.481	.323	-.367
(4) 601.8 - 614.2	-.467	-.534	-.434	.226	.435	.237	-.072	.058
(5) 646.2 - 660.4	-.142	-.083	.293	.169	-.061	-.319	-.694	.519
(6) 665.8 - 678.2	.371	.268	-.547	.466	.199	-.482	-.018	.004
(7) 746.1 - 749.7	-.522	.504	.067	-.339	.493	-.322	.068	-.037
(8) 871.4 - 878.6	.494	-.465	.195	-.400	.515	-.273	.009	-.013

Table 6.4. The eigenvectors of the covariance matrix from the Island View image.

	Eigenvector (Component) Number							
Bandwidths (nanometers)	1	2	3	4	5	6	7	8
(1) 431.6 - 459.4	.460	.465	.391	.357	.340	.320	.119	.240
(2) 480.3 - 499.6	-.596	-.411	.243	.293	.125	.304	.197	.426
(3) 545.3 - 559.4	-.216	.002	.146	.187	.234	.222	.247	-.855
(4) 601.8 - 614.2	.426	-.387	-.374	-.042	.061	.074	.716	.061
(5) 646.2 - 660.4	-.417	.656	-.133	-.200	-.164	-.088	.534	.127
(6) 665.8 - 678.2	-.161	.145	-.678	.030	.616	.198	-.258	.077
(7) 746.1 - 749.7	-.045	-.099	.331	-.321	.631	-.597	.130	.053
(8) 871.4 - 878.6	-.031	.043	-.198	.778	-.062	-.588	.051	-.010

Table 6.5. The squared loadings of the eigenvectors of the covariance matrix from the Sidney image.

	Eigenvector (Component) Number							
Bandwidths (nanometers)	1	2	3	4	5	6	7	8
(1) 431.6 - 459.4	.023	.040	.168	.189	.164	.117	.120	.179
(2) 480.3 - 499.6	.013	.029	.049	.052	.079	.081	.282	.411
(3) 545.3 - 559.4	.070	.094	.167	.186	.013	.231	.104	.135
(4) 601.8 - 614.2	.219	.285	.188	.051	.189	.057	.005	.003
(5) 646.2 - 660.4	.021	.009	.085	.029	.004	.102	.482	.270
(6) 665.8 - 678.2	.138	.072	.300	.218	.040	.232	.000	.000
(7) 746.1 - 749.7	.271	.254	.004	.114	.245	.104	.005	.001
(8) 871.4 - 878.6	.244	.216	.038	.160	.265	.074	.000	.000

Table 6.6. The squared loadings of the eigenvectors of the covariance matrix from the Island View image.

	Eigenvector (Component) Number							
Bandwidths (nanometers)	1	2	3	4	5	6	7	8
(1) 431.6 - 459.4	.212	.217	.152	.127	.116	.102	.014	.058
(2) 480.3 - 499.6	.355	.169	.059	.086	.015	.092	.038	.181
(3) 545.3 - 559.4	.047	.000	.021	.035	.055	.049	.061	.731
(4) 601.8 - 614.2	.181	.149	.140	.002	.004	.005	.513	.004
(5) 646.2 - 660.4	.174	.430	.018	.040	.027	.008	.286	.016
(6) 665.8 - 678.2	.026	.022	.460	.001	.379	.040	.067	.006
(7) 746.1 - 749.7	.002	.010	.110	.102	.398	.358	.017	.002
(8) 871.4 - 878.6	.001	.002	.039	.605	.004	.346	.003	.000

Table 6.7. Eigenchannel (component) and Percent Variance for the Sidney Image.

Eigenchannel	Percent Variance
1	86.82
2	12.01
3	0.59
4	0.29
5	0.20
6	0.07
7	0.02
8	0.01

Table 6.8. Eigenchannel (component) and Percent Variance for the Island View Image.

Eigenchannel	Percent Variance
1	88.99
2	4.18
3	3.24
4	1.50
5	0.82
6	0.66
7	0.40
8	0.22

The initial component images were generated using both the land and marine areas of the Sidney and Island View scenes, but high reflectance and wide variation in the spectral properties of the land accounted for over 95 percent of the variance in the first component for both images. Most of the information pertaining to the intertidal environment was found in the fifth through eighth components, where analysis became difficult as most of the useful intertidal information as well as noise was compressed into three or four component images. This problem was corrected by masking out the land areas.

All eight input bands were used in the PCA, and eight component images were generated. Loadings from each eigenvector were used to find the squared loadings of the eigenvectors, which explain the percentage of variance that each input band explains in each component (Tables 6.5 - 6.6) (Jensen 1986, Johnston 1980, Richards 1986). The squared eigenvectors for both the Sidney and Island View datasets will be compared in hopes to identify similar input bands that discriminate between intertidal vegetation in both images.

6.5.1. *Vegetation*

When the eight component images were generated, it was found that the first component delineated the land-water (intertidal-subtidal) boundary and little else, while the second component highlighted the presence/absence of vegetation, which is also of limited use considering the abundance of information contained in the other components. Component three highlighted certain algal genera, but not others. Component image four of both data sets, however, could be used for the identification of intertidal vegetation, as Chlorophytes appear dark or lighter (depending on genera), Phaeophytes light, and

substrates grey. Component images five through eight contained large amounts of noise which made vegetation identification more difficult than using component four.

An examination of the squared eigenvectors for component four shows that bands 1, 3, 6 and 8 contribute the greatest loadings for the Sidney image, and bands 1 and 8 for the Island View image (Tables 6.3 - 6.4). The relationships between bands and component images are discussed below.

Band 1 (431.6 - 459.4 nm) contributed significant amounts of information to those components where the differences in vegetated and non-vegetated areas were apparent. The high information content of band 1 is most likely due to chlorophyll and fucoxanthrin absorption in the 430-460 nm wavelengths (Rowan 1989). Less algal cover in the Island View scene may be one reason why band 1 loadings are not as large as the loadings in the Sidney image for the fourth component.

Band 2 (480.3 - 499.6 nm) contributed small amounts of information for both scenes, but may be useful as the spectral region was selected for discrimination between chlorophylls *a* and *b* which may aid in Chlorophyte identification (Kirk 1983, Rowan 1989).

Band 3 (545.3 - 559.4 nm) is similar to band 1 in that high component loadings were recorded for the Sidney image and lower loadings for the Island View image. The high loading on band 3 of the Sidney image may be caused by the presence of carotenoid pigments in *Fucus distichus*, which are photosynthetically active in the green regions of the spectrum. There are no areas of *Fucus distichus* larger than 1 square meter on Island View Beach, therefore the band 3 would only contain information on the Chlorophytes in the Island View scene. The information contained in band 3 would also be available in other bands, therefore band 3 does not contribute large amounts of essential information for intertidal identification on the Island View image. Band 3 may be valuable in the identification of Rhodophytes (red algae), but significant amounts of these algae were not present in either scene to test this hypothesis (Carefoot 1983, Rowan 1989).

Bands 4 and 5 contribute little information in both scenes. Band 4 (601.8 - 614.2 nm) was added to the bandset to detect biliproteins, which are present in the Rhodophyceae, but neither study site contained significant amounts of Rhodophytes (Glazer 1981). Band 5 (646.2 - 660.4 nm) was selected for chlorophyll *b* identification and to bridge the bandset between bands 4 and 6 (Kirk 1983, Rowan 1989).

Band 6 (665.8 - 678.2 nm) contributed the most information to component four in the Sidney image, but the least information to component four of the Island View image. This characteristic may be due to the differences in biomass between the two study sites. Correlations (Tables 6.1 - 6.1) between band 6 and the NIR bands are the weakest for the visible bands of the Sidney image, whereas the degree of association between band 6 and the NIR is the highest among the visible bands for the Island View image. As the spectral reflectance for substrates generally exhibits similar reflectances throughout the visible and NIR, it would follow that the red regions would be highly correlated with the NIR (as seen in the Island View image). As biomass increases, and contributions from substrates to overall spectral reflectance decrease, correlations between red and NIR would decrease, as seen in the Sidney image (Tables 6.1 - 6.2).

The spectral regions that appear to contribute the greatest to vegetation identification are bands 1, 3, 6, 7, and 8. As the NIR bands are better used in the detection rather than identification of vegetation (see previous section), only band 8 was selected for the "best" choice bands for classification, which include bands 1, 3, 6, and 8. The following section will classify this reduced bandset and compare the results with classified images created using various combinations of bands.

6.5.2. *Substrates*

Substrate identification proved difficult in the Sidney image as vegetation obscured certain substrates. The PCA images generated above were used to determine which

component images best differentiated substrates. The component loadings were again examined to determine how each band contributed to substrate identification (Tables 6.5 - 6.6).

Components three, four and five highlighted the differences between substrates in the Sidney image, where component three could be used to differentiate between submerged and emerged sands as well as muds and gravels. The visible bands, particularly bands 1, 3, 4 and 6 contributed the most information to component three. Component four highlighted the differences between submerged substrates and loaded heavily on bands 1, 3 and 6, and to a lesser extent bands 7 and 8 in the NIR. Submerged vegetation and substrates were highlighted in component five, where bands 1, 4, 7 and 8 contributed the greatest variance. The reason for the clear distinction between substrates and vegetation in this component may be due to NIR penetration into the water where upright aquatic vegetation near the surface reflects these wavelengths. NIR radiation that is not reflected from vegetation may be attenuated as it travels towards the benthos, or attenuated when scattered or reflected toward the surface.

Components two, four and five could be used to identify different substrates in the Island View Image. For all components, bands 1, 5, 6, 7 and 8 contributed the most variance to those components where substrates could be differentiated. The bands contributing to substrate identification that are common to both the Sidney and Island View images are bands 1, 7 and 8. These bands were also found above to be important in vegetation detection and identification, therefore the bandset consisting of bands 1, 3, 6, 7 and 8 which were found above to be best suited for vegetation identification can also be used in substrate discrimination.

6.6. Conclusions

Results from the PCA when applied to vegetation identification are promising. Using a single component image, Chlorophytes could be distinguished from Phaeophytes and all emerged vegetation could be separated from substrates. Identification of substrates proved more difficult as vegetation obscured much of the intertidal region, but muds, sands and gravels could be differentiated where algal cover is scarce.

The results of this study compare favorably with those of Budd & Milton (1982), as both studies found that the information pertaining to intertidal vegetation identification was contained in a component containing a small proportion of the total variance for the scenes. Budd & Milton (1982) found that component image three best discriminated between genera, whereas this research found component four to be better. Component four contributed 0.29 percent of the total image variance for the Sidney scene, and 1.5 percent of the variance for the Island View image.

The difference in components used between the two studies is due to Budd & Milton's (1982) use of a handheld spectroradiometer, which did not image marine areas. The imagery included in this study, however, included marine areas which were delineated from the littoral regions in the first component and consequently the third component in Budd & Milton's (1982) study became the fourth component in this research. The presence of sublittoral regions in the imagery of this study may also account for the slightly higher percentage of the trace that component three contributes in Budd & Milton's research (Budd & Milton 1982).

In conclusion, as the amount of image variance that contributes to the identification of vegetation and substrates is very small (Tables 6.7 - 6.8), therefore PCA images may be valuable in the classification of the imagery, as they are a method of eliminating unwanted information that does not contribute to vegetation and substrate discrimination.

CHAPTER 7

CLASSIFICATION OF THE IMAGERY

7.1. Introduction

To determine the usefulness of the multispectral imagery for intertidal vegetation and substrate identification, both the Sidney and Island View data sets were classified, and the resulting classifications compared to the field data to establish classification accuracies. As the purpose of this research is to determine if multispectral imagery can be used to identify vegetation and substrates, rather than map land cover types, unsupervised classifications were selected over supervised techniques. Unsupervised classifications were chosen for clustering image data so as to establish "natural" groupings, or clusters in the data (Jensen 1986, Richards 1986). Determining the natural groupings of the data yields some notions as to how many distinct classes can be separated and how to determine the accuracy of these classifications.

The Sidney and Island View images were classified using an unsupervised clustering algorithm based on the ISODATA algorithm described by Tou &Gonzales (1974). The ISODATA classifier is an iterative routine similar to the more popular K-means, but includes heuristic procedures to assist in identifying cluster centres. The decision to use the ISODATA algorithm was dictated by the imaging processing software available for this research, and the knowledge that the routine is fairly sophisticated but does not require extensive processing time. The ISODATA routine also gives the user the option to *a priori* input the desired number of final classes, which is useful when the approximate number of major cover types is known. Several other unsupervised algorithms were initially used in this study, but found to be inferior to the ISODATA classifier as classifications were not as accurate as the ISODATA routine when compared with *in situ* fieldwork.

The methodology used in classifying the imagery was essentially trial and error, as previous research in intertidal remote sensing uses mainly the Landsat bands, which have different locations and widths in the spectrum compared to the bands used in this study. Consequently, several different strategies were employed in classification of the imagery, in hopes to find bands, or combinations of bands that adequately represent reality. The strategies employed in searching for acceptable classifications included; a) using all bands, b) using certain bands, c) using band ratios in classification, and d) using PCA images in classification.

7.2. Classification of the Imagery: Vegetation

Classification of the imagery proved more challenging than anticipated as classifications that included the NIR bands did not differentiate between algal genera, but rather yielded areas of different algal density (biomass). Classifications that excluded the NIR bands could not be used for intertidal vegetation mapping as algal genera were indistinguishable from substrates in the classified images. As classification of visible bands and the visible bands plus the NIR bands yielded poor results, different combinations of channels were used. After much experimentation, bands 1, 3, 6 and 8, which were found in Chapter 6 to contain the most information related to vegetation identification, resulted in classified images where Phaeophytes could be distinguished from Chlorophytes, but all Chlorophytes were assigned to the same class. No amount of band manipulations could separate the spectrally similar Chlorophytes, nor did changing the parameters of the classification, such as adding more clusters or changing the probabilities of a cluster being included into a class. The use of band ratios also did not separate the Chlorophyte genera, and neither did the use of combinations of band ratios and raw imagery.

The only classifications of any value for intertidal seaweed identification were those created using PCA images as input bands. The best classification for the Sidney image was created using PC2, PC3 and PC4 created from a PCA using bands 1, 2, 3, 6 and 8 (Figure 7.1). Although band 2 appeared to contribute little to species identification in the PCA, differentiation between Chlorophytes was only possible when band 2 was included in the creation of PCA images which were later classified. The region is sensitive to varying ratios of chlorophyll *a* and *b*, and certain carotenoids, which may be the reason the band 2 is needed for Chlorophyte identification (Kirk 1983, Rowan 1989). Substrates in Figures 7.1 and 7.2 have been shaded a single colour for ease of identification.

As there was only one genera of intertidal vegetation in the Island View image (*Monostroma spp.*), bands 1, 2, 3, 6 and 8 or the PCA images created using bands 1, 2, 3, 6 and 8 adequately classified areas of this genera (Figure 7.2). The nearshore *Nereocystis* beds were easily classified using the NIR bands, as floating vegetation strongly reflects in the NIR regions while water absorbs most of these wavelengths. As there was no field sampling of the beds during imaging, there is no method to evaluate classification accuracies, therefore the nearshore beds are excluded from the following classification and accuracy assessment.

7.3. Classification of the Imagery: Substrates

Classification of substrates was only difficult when vegetation covered the surface. As there was no way of eliminating the presence of vegetation from the imagery, the only method of identifying obscured substrates was to use the species as an indicator of substrates (ie. *Fucus spp.* generally covers upper intertidal rock substrates) (Scagel 1961).

Figure 7.1. An unsupervised classification of the Sidney image using principle components two, three and four from a PCA created with bands 1, 2, 3, 6 and 8. Areas of red are *Fucus distichus*, green are *Enteromorpha spp.* and/or mixed Chlorophytes, purple areas are beds of the Chlorophyte *Blidingia spp.* Green areas along the waterline of Sidney Shore are areas of the Chlorophyte *Monostroma spp.* Brown areas are organic rich muds with sparse areas of Chlorophytes covering them. Boxes A and B are areas where an accuracy assessment was performed.

Figure 7.2. An unsupervised classification of the Island View image using principle components 2, 3 and 4 created with bands 1, 2, 3, 6 and 8. Areas of red are *Monostroma spp*. and the boxed area indicates where the accuracy assessment was performed.

Many different combinations of bands were useful in identifying substrates. No special combination(s) of bands, ratios and components were needed. The use of PC1, PC2 and PC3 was useful for both the Sidney and Island View images in discriminating between substrates, especially between submerged and emerged materials, but if vegetation has not been previously mapped, there may be some vegetation classified as substrates. The optimal method for classifying substrates was
to classify the vegetation first, then examine areas not identified as vegetation. This technique was found to be the most efficient method as a) vegetation was not misclassified as substrates, and b) the species of vegetation may be used as an indicator as to underlying substrates. Figures 7.3 and 7.4 illustrate the different substrates with all vegetation combined into one class to facilitate identification of substrates.

7.4. Accuracy Assessment

The accuracy of the classifications was assessed by comparing the classifications produced using the ISODATA unsupervised clustering algorithm with *in situ* field data. Homogeneous training areas were identified using the video imagery, and subsequently transferred onto raster bitmaps that could be used to overlay the classified imagery. This process was accomplished by examining the video imagery and determining the extents of algal and substrate regions, which were then traced onto the imagery using a cursor. Pixel counts under the bitmaps are shown in Tables 7.1 - 7.5. Although this video-to-image method is less rigorous than pure transect sampling, collecting field data using the transect method was not feasible during imaging due to the number of sites imaged and a short low tide window (see Chapter 5).

Accuracy assessment was performed only on areas where accurate fieldwork was obtained, and on areas which contained homogeneous areas of vegetation and substrates.

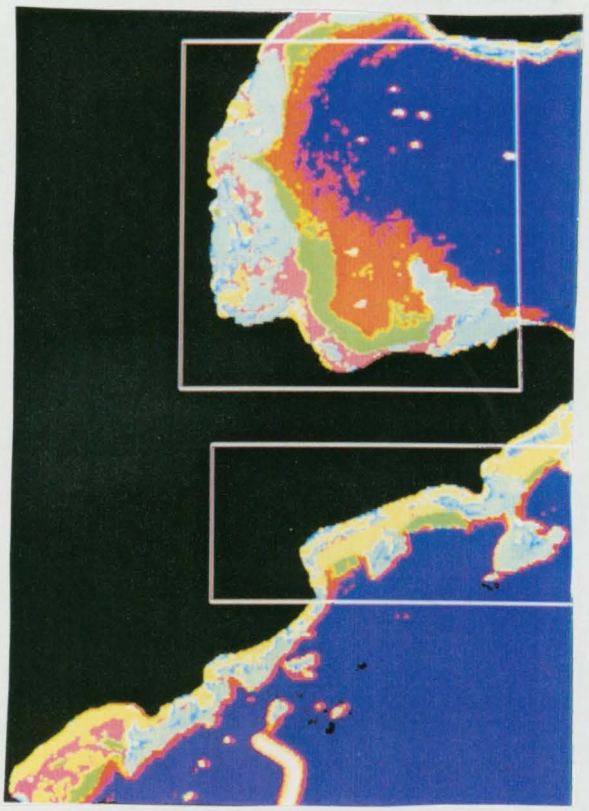

Figure 7.3. An unsupervised classification of the Sidney image using principle components 2, 3 and 4 created with bands 1, 2, 3, 6 and 8. Purple areas indicate exposed organic rich muds/sands, green areas are slightly submerged muds, orange regions are submerged muds, blue areas are dry sands and yellow regions are organic poor muds and sands. Grey regions are vegetative cover.

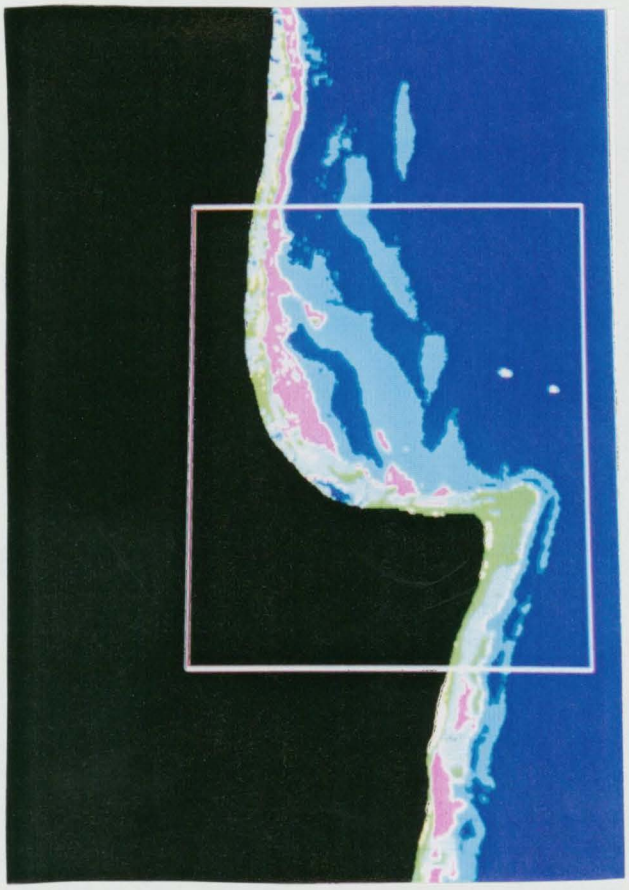

Figure 7.4. An unsupervised classification of the Island View image using principle components 2, 3 and 4 created with bands 1, 2, 3, 6 and 8. Green areas indicate cobble/gravel substrates, pink areas are wet sands and muds and blue areas are dry sands.

Several regions in the Sidney image were composed of up to 10 genera of algae, therefore these areas were not used in determining classification accuracy.

7.4.1. *Vegetation*

Two regions of the Sidney image were assessed for classification accuracy, while one area of the Island View image was used (Figures 7.1 - 7.2). Two distinct physical shoreline types are represented in the Sidney image (Roberts Bay muds and Sidney Shore bedrock, sands and muds), therefore the image was separated into two regions which were classified separately.

Classification of *Blidingia* and *Enteromorpha* beds in Roberts Bay were quite accurate (86%), considering these algae are spectrally similar (Table 7.1). One reason these genera could be differentiated may be the presence of small amounts of *Pilayella* (brown algae) found in conjunction with the *Enteromorpha.* The density of *Pilayella* varied throughout the *Enteromorpha* beds, however, and was not ubiquitous.

Classification of *Fucus distichus* and *Monostroma* on the Sidney Shore regions was not as accurate as those in Roberts Bay (65%) (Table 7.2). This is most likely due to smaller, and consequently less accurate training areas, and areas where *Fucus* and *Monostroma* occur together.

An accuracy assessment of the Island View image found that 74% percent of the *Monostroma* in the scene was correctly classified (Table 7.3). Classification accuracies for the three sites may appear low when compared to classification accuracies obtained using satellite imagery, but this number may be low due to a) qualitative judgements when mapping training sites using data obtained from a hand-held video camera and b) the high spatial resolution of the data in which small differences in the density of the vegetative cover may be evident as differently classed pixels.

Table 7.1. Pixel counts and classification accuracy for Roberts Bay vegetation. Pixel counts from classified imagery are plotted along the Y direction of this table.

Genera	*Blidingia*	*Enteromorpha(Pilayella)*
Blidingia	1089	622
Enteromorpha (Pilayella)	42	4537
Other	18	215

Correctly classified = 5626/6523 = 0.862 = 86 percent.

Table 7.2. Pixel counts and classification accuracy for Sidney Shore vegetation.

Genera	*Fucus*	*Monostroma*
Fucus	390	99
Monostroma	159	495
Other	47	166

Correctly classified = 885/1356 = 0.653 = 65 percent.

Table 7.3. Pixel counts and classification accuracy for Island View beach vegetation.

Genera	*Monostroma*
Monostroma	576
Other	204

Correctly classified = 576/780 = 0.738= 74 percent.

7.4.2. *Substrates*

The procedure used above to assess the accuracy of the vegetation classifications was also used for the substrates. Roberts Bay and Sidney Shore, however, were evaluated together, as similar substrates were present in each region. As vegetation obscured much of the surface cover in the Sidney image, classification accuracies are low (Table 7.4). The non-vegetated mud/sand areas of Sidney Shore, however have significantly higher classification accuracies.

Classifications for the Island View image were much more accurate as most intertidal areas either lacked an algal cover or were host to sparse communities. A *Monostroma* community was supported by gravel/sand substrates in the lower intertidal regions, and as a result, classification accuracies were poor (Table 7.5). Classifications of cobbles, sands and muds lacking organic cover, however, were quite accurate with the exception that cobbles are spectrally similar to the mixed substrate regions, which decreased classification accuracies (Table 7.5).

Table 7.4. Pixel counts and classification accuracy for Roberts Bay and Sidney Shore substrates. Pixel counts from the classified imagery are plotted along the Y direction of this table.

Substrate	Muds/Sands	Sands/Gravels	Bedrock
Muds/Sands	810	148	49
Sands/Gravels	0	232	13
Bedrock	10	121	18
Other	303	16	0

Correctly classified Muds/Sands = 810/1123 = 0.72 = 72%
Sands/Gravels = 232/517 = 0.45 = 45%
Bedrock = 18/80 = 0.23 = 23%

Table 7.5. Pixel counts and classification accuracy for Island View Beach substrates.

Substrate	Cobbles	Upper Sands	Lower Sands/Gravels	Muds
Cobbles	275			
Upper Sands		133	1	
Lower Sands			34	
Muds				242
Mixed Substrates	111	4		33
Vegetation	9	1	75	2
Water			1	17

Correctly classified Cobbles = 275/395 = 0.70 = 70%
Upper Sands = 133/138 = 0.96 = 96%
Lower Sands = 34/111 = 0.31 = 31%
Muds = 242/294 = 0.82 = 82%

CHAPTER 8
CONCLUSIONS

Although there are several notable conclusions presented in this research, perhaps the most significant concerns the ability to differentiate between spectrally similar algal genera of the same taxonomic class (Chlorophyceae). Previous research has demonstrated the ability of remote sensing techniques to discriminate between the different classes and the estimation of algal biomass, but this is the first study of its kind to accurately differentiate between genera using imagery that could easily be incorporated into a coastal mapping framework (Budd & Milton 1982, Donoghue & Shennan 1987, Gross *et al.* 1985, Zibordi *et al.* 1990). Classification accuracies for vegetation ranged from 65% to 86%, where areas of mixed vegetation contributed to the lower accuracies. This thesis has not used specialized post-classification sorting techniques such as context sensitive filtering, but these techniques may be useful for improving results. Classification accuracies for substrates are generally lower (31% to 82%) than those for vegetation due to the presence of vegetation obscuring substrates. Again, if context sensitive routines were incorporated into the classification (i.e. the presence of *Fucus spp.* indicates bedrock substrates) accuracies may be improved.

This research also uses an unsupervised approach to classification, with no *a priori* input as to the spectral properties of the intertidal environment. If large areas of a shoreline are to be mapped, a database of spectral signatures could be created using either a portable spectrometer in the field or high spectral resolution data (i.e. the CASI in spectral mode). This technique may yield more accurate classification accuracies than strict unsupervised classification.

The conclusions of this research also indicate that algae and substrates can be accurately mapped using a multispectral bandset consisting of as few as 5 bands comprising the visible and NIR. The demonstration that a limited number of spectral

regions can be used to map coastal areas may influence or shape remote sensing trends leaning toward high spectral resolution coastal studies (O'Neill *et al.* 1988, Staenz 1992). This study also reinforces the limitations of the NIR regions in intertidal remote sensing, as the presence of moisture hampers algal and substrate identification using this region of the spectrum.

The PCA was found to be a useful tool for identifying spectral information contributing to the discrimination of intertidal features and phenomena. The technique also permitted some insight as to which bands are best suited for coastal remote sensing, and yielded a method for dealing with the dominance of the NIR wavelengths when using these regions for classification. As a result, the PCA is a valuable tool in both exploration and classification of imagery obtained in intertidal and nearshore areas.

The bandset selected for this study proved adequate for classifying vegetation and substrates, although future research may benefit from certain changes. The most notable change to the bandset would be the deletion or merging of bands four and five (red), as they are highly correlated and contribute little to vegetation and substrate identification. For vegetation identification, a single NIR band proved adequate as the presence of water limited the usefulness of these spectral regions. If the bandset was to be used for biomass estimation, the addition of other NIR and middle IR regions may be useful (Bartlett & Klemas 1981, Gross *et al.* 1985). A bandset created for intertidal mapping ideally should contain a minimum of four bands, which include the blue regions for chlorophyll absorption and clear water penetration, green regions for the detection of Chlorophytes and penetration of murky waters, a red band for chlorophyll absorption and the differentiation of vegetation from substrates, and lastly a NIR band for detecting vegetation and moisture in the littoral environment.

The conclusions reached in this study may not be identical to results of other research, as the results obtained in this study are a direct consequence of the multispectral bandset selected, the time of imaging (day and season), the spatial resolution (flight

height), and the performance characteristics of the CASI. Another study using a different bandset, or imaging in winter for instance, may derive different results and conclusions than this study. The likelihood of this scenario occurring, however, is remote as the bandset chosen in this study approximates the spectral regions most likely to detect the physical, chemical and biological processes that differentiate between intertidal features and phenomena using the visible and NIR regions of the spectrum. Mapping vegetation is best accomplished in late summer and early fall, as absolute littoral biomass has peaked during these months (Budd & Milton 1982, Gross *et al.* 1985). As a result, vegetation classifications may have been slightly more accurate if the sites were imaged later in the year. Conversely, the winter months may have yielded better substrate classifications as vegetation is significantly reduced in contrast to summer. Substrate classifications may also be different in the winter months as winter storms tend to transport smaller materials offshore (Moore & Seed 1986).

This research has demonstrated that accurate intertidal vegetation and substrate surveys are possible using airborne remotely sensed data. The next step in this research is to use airborne multispectral data to classify the shoreline into and existing habitat classification scheme used by agencies that are involved in coastal management. Ideally, an automated routine would be developed that calculates the areal and percentage cover for both vegetation and substrates, and using this information, fits the shoreline into an existing habitat classification system. This routine could provide a powerful tool for the automated mapping and habitat classification for large areas of coastline. Investigation into using airborne multispectral data to classify shoreline habitats is currently being studied by both the provincial Ministry of Environment, Lands and Parks and the federal Department of Fisheries and Oceans (DFO).

As the intertidal and nearshore environments along the coast of British Columbia become increasingly threatened by human activities, there is a need for accurate and current data to effectively manage and protect coastal areas. New technologies, such as imaging

spectrometry, offer the means to gain a better understanding of the biophysical properties and phenomena associated with coastal environments. Imaging spectrometry has the potential to provide a powerful and flexible tool that may substantially increase the knowledge of the world's coastal resources, as well as provide a tool for the periodic monitoring and mapping of these regions. The flexibility of airborne systems also allows rapid deployment of this technology for use in marine and terrestrial accidents that affect coastlines.

The use of imaging spectrometry for oil spill contingency planning and as a tool to assess spill damage is a reactive solution to the threat of marine accidents. Reactive solutions, however, are currently the most politically viable options to minimize damage from spills, and remotely sensed data may be instrumental in assessing the environmental damage and potential economic loss due to an accident. Currently, the lack of detailed information concerning our coastlines hinders the possibility of compensation for those whose livelihood depends on the coastal environment (ie. Native fisheries), as it is difficult to claim damages for an affected habitat such as a kelp forest if there was no documented record of the forest prior to the accident.

The CASI and other similar technologies are merely research tools at this point in time, but may become instrumental in the future for monitoring and mapping areas considered to be unmanageable today. As these remote sensing techniques evolve, the costs of imagery will decrease and accessibility to this information will increase. The resulting detailed information on the state of our lands and waters will hopefully promote awareness and perhaps accountability as to how we as a people manage our environment.

Before the organizations and agencies who are involved with the health of our coasts will adopt these new technologies, however, it must be substantiated that there is either an economic incentive or increase in effectiveness over existing methods and techniques. Otherwise these technologies will remain research tools, which limits their real - world usefulness.

REFERENCES

Abbott, I.A. and G.J. Hollenberg, 1976. *Marine Algae of California*. Stanford Press, Stanford.

Anon - "Brotherhood slams governments inaction." *Kahtou*, 23 January 1989 p. 3.

Anon - "Hydrocarbons threaten coastal life." *Kahtou*, 23 January 1989 p. 2-3.

Ardanuay, P. E., D. Han and V.V. Salomonson, 1991. "The moderate resolution imaging spectrometer (MODIS) science and data system requirements." *IEEE Transactions on Geoscience and Remote Sensing* 29(1).

Augenstein, D.A., D.A. Stow and A.S. Hope, 1991. "Evaluation of SPOT HRV-XS Data for Kelp Resource Inventories." *Photogrammetric Engineering and Remote Sensing* 57(5).

Austin, A. and R. Adams, 1978. "Aerial colour and colour infrared survey of marine plant resources." *Photogrammetric Engineering and Remote Sensing* 44(4).

Avery, T.E. and G.L. Berlin, 1992. *Fundamentals of Remote Sensing and Image Interpretation*. Maxwell Macmillam, Toronto.

Bartlett, D.S. and V. Klemas, 1981. "In situ spectral reflectance studies of tidal wetland grasses." *Photogrammetric Engineering and Remote Sensing* 47.

Bennett, D.W. (editor), 1970. "202 questions for the endangered coastal zone." *Special Publication of the American Littoral Society,* Inc. 6(26).

Belsher, T. L. Loubersac and G. Belbeoch, 1983. "Teledetection et variations du phytobenthos intertidal." *Oceanoligica Acta*. Actes 17 Symposium Europeen Biologie Marine, Brest, 27 spetembre -1 octobre 1982.

Bhargava, D.S. and D.W. Mariam, 1990. "Spectral relationships to turbidity generated by different clay materials." *Photogrammetric Engineering and Remote Sensing* 56(2).

Bhargava, D.S. and D.W. Mariam, 1991. "Effects of suspended particle size and concentration on reflectance measurements." *Photogrammetric Engineering and Remote Sensing* 57(5).

Bold, H.C. and M.J. Wynne, 1987. *Introduction to the Algae*. Prentice-Hall, New Jersey.

Borstad, G.A., H.R. Edel, J.F.R. Gower and A. B. Hollinger, 1985. "Analysis of test and flight data from the fluorescence line imager." *Canadian Special Publication of Fisheries and Aquatic Sciences*. Vol. 83.

Borstad, G.A. and D. A. Hill, 1989. "Using visible range imaging spectrometers to map ocean phenomena." *Proceedings from the Advanced Optical Instrumentation for Remote Sensing of the Earth's Surface from Space*. Vol. 1129.

British Columbia Aquaculture Research and Development Council, 1990. *Aquaculture in B.C*. Province of British Columbia.

Budd, J.T.C. and E.J. Milton, 1982. "Remote sensing of salt-marsh vegetation in the first four proposed TM bands." *International Journal of Remote Sensing* 3.

Calabrese, A., F.P. Thurberg, F.J. Vernberg, W.B. Vernberg, 1987. *Pollution Physiology of Estuarine Organisms*. South Carolina, University of South Carolina Press.

Cameron, H.L., 1950. "The use of aerial photography in seaweed surveys." *Photogrammetric Engineering* 16.

Campbell, N.A., 1987. *Biology* . Benjamin/Cummings Inc., Don Mills Ont.

Canada, 1991. *Health of Our Oceans:A Status Report on Canadian Marine Envionmental Quality*. eds P.G. Wells and S.J. Rolston. Environment Canada, Dartmouth.

Canada, 1990. *Canadian Tide and Current Tables 1991*. Vol 5.

Canada, 1988. *Aquaculture in Canada*. Department of Fisheries and Oceans Government of Canada.

Carefoot, T., 1983. *Pacific Seashores: A Guide to Intertidal Ecology*. Douglas and McIntyre, Vancouver.

Chiu, H.Y. and W. Collins, 1978. A Spectroradiometer for Airborne Remote Sensing. *Photogrammetric Engineering and Remote Sensing* 44(4).

Clarke, G.L., G.C. Ewing and C.J. Lorenzen, 1970. "Spectra of backscattered light from the sea obtained from aircraft as a measure of chlorophyll concentration." *Science* 167.

Currant, I.B., 1969. "A blue-insensitive anscochrome aerial film." *Papers from the 35th Annual Meeting of the American Sociey of Photogrammetry.*

Dayton, P.K., 1975. "Experimental evaluation of ecological dominance in a rocky intertidal algal community." *Ecological Monographs* 45.

Dethier, M. N., 1982. "Pattern and process in tidepool algae: factors influencing seasonality and distribution." *Botanica Marina* 25.

Dera, J., 1992. *Marine Physics.* Elsevier, New York.

Dickens, D., H. Rueggeberg, M. Poulin, I. Bjerklund, J. Haggarty, L. Solsberg, J. Harper, A. Godon, D.Reimer, J. Booth, and K. Neary, 1990. *Oil Spill Response Atlas for the Southwest Coast of Vancouver Island.* BC Environment, Province of British Columbia.

Dold, Catherine. "Weighing the cost of saving wildlife." *The Vancouver Sun,* 4 January 1992 p. B6.

Donoghue, N.M. and Ian Shennan, 1987. "A Preliminary assessment of Landsat TM imagery for mapping vegetation and sediment distribution in the Wash Estuary." *International Journal of Remote Sensing* 8(7).

Druel, L.D. and J.M. Green, 1982. "Vertical distribution of intertidal seaweeds as related to patterns of submersion and emersion." *Marine Ecology Progress Series* 9.

Egle, K., 1960. "Menge und verhaltnis der pigmente." *Encyclopedia of Plant Physiology* ed. W. Ruhlanf, vol 5. Springer-Verlag, Berlin.

Elachi, C., 1987. *Introduction to the Physics and Techniques of Remote Sensing.* John Wiley and Sons, New York.

Ferrier, G. and J.M. Anderson, 1990. "Remote sensing observations of the Tay Estuary, Scotland." *Remote Sensing Science for the Nineties: 10th Annual Geoscience and Remote Sensing Symposium.*

Fogg, G.E. and B.Thake, 1987. *Algal Cultures and Phytoplankton Ecology.* University of Wisconsin Press.

Gates, D.M., H.J. Keegan, J.C. Schleter and V.R. Weidner, 1965. "Spectral properties of plants." *Applied Optics* 4(1).

Glazer, A.N., 1981. "Photosynthetic accessory proteins with bilin prosthetic groups." *The Biochemistry of Plants*, vol 8 Academic Press, New York.

Goetz, A.F.H and M.Herring, 1989. The high resolution imaging spectrometer(HIRIS) for EOS. *IEEE Transactions on Geoscience and Remote Sensing* 27(2).

Gower, J.F.R. and G.A. Borstad, 1990. "Mapping of phytoplankton by solar-stimulated fluorescence using an imaging spectrometer." *International Journal of Remote Sensing* 11(2).

Gower, J.F.R, S. Lin and G.A. Borstad, 1984. "The information content of different optical spectral ranges for remote chlorophyll estimation in coastal waters." *International Journal of Remote Sensing* 5(2).

Grimes, B.H. and J.C.E. Hubbard., 1971. "A comparison of film type and the importance of season for interpretation of coastal marshland vegetation."

Gross, M.F., V. Klemas and J.E. Levasseur, 1985. "Remote sensing of spartina anglica biomass in five French salt marshes." *International Journal of Remote Sensing* 7(5).

Hardisky, M.A, F.C Daiber, C.T. Roman and V. Klemas, 1984. "Remote sensing of biomass and annual net aerial primary productivity of a salt marsh." *Remote Sensing of the Enivironment* 16.

Hilton, J., 1984. "Airborne Remote Sensing for Freshwater and Estuarine Monitoring." *Water Resources.* 18(10).

Hobbs, A.J. and I. Shennan, 1986. "Remote sensing of salt marsh reclaimation in the Wash, England." *Journal of Coastal Research* 2(2).

Hodgson, R.M., F.M. Cady and D. Pairman, 1981. "A solid state airborne sensing system for remote sensing." *Photogrammetric Engineering and Remote Sensing* (2).

Hruby, T., 1976. "Observations of algal zonation resulting from competition." *Estuarine and Coastal Marine Science* 4.

Hunter, R. A., L. E. Jones, M. M. Wayne and B. A. Pendergast, 1983. "Estuarine habitat mapping and classification system manual." *MOE Manual* (3).

Hume, J. "Oil greater threat than sewage." *Times Colonist* [Victoria], 27 November 1992 p. A3.

Jamison, D.W., 1972. "Aerial remote sensing as a tool in seaweed surveys."*Proceedings of the International Seaweed Symposium* VII. Univ. Tokyo Press, Tokyo.

Jensen, Arne and Bent Lorenzen, 1988. "Reflectance of blue, green, red, and near infared from wetland vegetation used in a model discriminating live and dead above ground biomass." *New Phytologist* 108.

Jensen, J. R., 1986. *Introductory Digital. Image Processing*. New Jersey, Simon and Schuster.

Jensen, J.R., J.E. Estes and L.Tinney, 1980. "Remote sensing techniques for kelp surveys." *Photogrammetric Engineering and Remote Sensing* 46(6).

Johnston, R.J., 1980. *Multivariate Statistical Analysis in Geography*. New York, Longman.

Kapetsky, J. M., L. McGregor and H. Nanne E, 1987. "A geographical information system and satellite remote sensing to plan for aquaculture development: a FAO-UNEP/GRID cooperative study in Costa Rica." *FAO Fisheries Technical Paper 287*.

Kelly, M.G. and A. Conrod, 1969. *Remote Sensing in Ecology* ed. P.L. Johnson. Univ. Georgia Press, Athens.

Khan, M.A., Y.H. Fadlallah and K.G. Al-Hinai, 1992. "Thematic mapping of subtidal coastal habitats in the western Arabian Gulf using Landsat TM data - Abu Ali Bay, Saudi Arabia.

Kirk, J.T.O., 1983. *Light and Photosynthesis in Aquatic Ecosystems*. Cambridge Press, New York.

Kopelevich, O.V. and V.I. Burrnkov, 1977. "Relation between the spectral values of the light absorption coefficients of sea water, phytoplanktonic pigments, and the yellow substance." *Oceanology* 17.

Kozloff, E.N., 1983. *Seashore Life of the Northern Pacific Coast* . Douglas and McIntyre, Vancouver.

Kruse, F.A., 1991. "Mineral mapping at Cuprite, Nevada with a 63 channel imaging spectrometer." *Photogrammetric Engineering and Remote Sensing* 56(1).

Lee, R.E., 1989. *Phycology*. Cambridge Press, New York.

Lee, W.T., 1922. "The face of the earth as seen from the air." *American Geographical Society*.

Lepley, L.K. 1968. "Coastal water clarity from space photographs." *Photogrammetric Engineering and Remote Sensing* 38(4).

Lockwood, A.P.M., 1976. *Effects of Pollutants on Aquatic Organisms*. London,Cambridge University Press.

Lukens, J.E., 1968. "Color aerial photography for aquatic vegetation surveys." *Proceedings of the Fifth Symposium on Remote Sensing of the Environment* University of Michigan

Luning, K., 1981. "Light." *The Biology of Seaweeds*. eds. S. Lobbon and M.J. Wynne,University of California Press, Berkley.

McConnaughey, B. H. and E. McConnaughey, 1986. *Pacific Coast*. Alfred A. Knopf, New York.

McKim, H.L., C.J. Merry and R.W. Layman, 1984. "Water quality monitoring using an airborne spectroradiometer." *Photogrammetric Engineering and Remote Sensing* 50(3).

Meulstee, C., P.H. Nienuis and H.T.C. Van Stokkom, 1988. "Aerial photography for biomass assessment in the intertidal zone." *International Journal of Remote Sensing* 9(10-11).

Moore, P.G. and R. Seed, 1986. *The Ecology of Rocky Coasts*. New York, Columbia University Press.

Neville, R. A. and J.F.R. Gower, 1977. "Passive remote sensing of phytoplankton via chlorophyll *a* fluorescence." *Journal of Geophysical Research* 82(24)

Obee, B., 1989. "Oil spill aftermath." *Canadian Geographic*. April/May 1989.

Odum, E.P., 1989. *Ecology and Our Endangered Life-Support Systems*. Sunderland, Sinauer Associates Inc.

Olson, D.P., 1964. "The use of aerial photographs in the studies of marsh vegetation." *Maine Agricultural Experimental Station Technical Bulletin* 13.

O'Neill. N.T., Y. Gauthier, E. Lambert, L. Hubert, J.M.M. Duboise, H.R. Edel and Y. Simard. 1988. "Imaging spectrometry applied to the remote sensing of submerged seaweed," *4th Colloque international sur les signatures spectrales d'objects en teledetection,* Aussois France.

Pan, D., J.F.R. Gower and G.A. Borstad, 1988. "Seasonal variation of the surface chlorophyll distribution along the British Columbia coast as shown by CZCS imagery." *Limnology and Oceanography* 33(2).

Porter, W.M. and H.T. Enmark, 1987. "A system overview of the Airborne Visible/Infared Imaging Spectrometer (AVIRIS)." *Imaging Spectroscopy II August '87* SPIE.

Quin, H. "Deadly coastal spills: oil slicks are threatening both coasts." *Maclean's*, 23 January 1989 p. 17.

Ragan, M.A., 1981. "Chemical constituents of seaweeds." *The Biology of Seaweeds*. eds. S. Lobbon and M.J. Wynne, University of California Press, Berkley.

Ramus, J., 1981. "The capture and transduction of light energy." *The Biology of Seaweeds*. eds. S. Lobbon and M.J. Wynne, University of California Press, Berkley.

Ramus, J. and G. Rosenberg, 1980. "Diurnal photosynthetic performance of seaweeds measured under natural conditions." *Marine Biology* 56.

Richards, J.A., 1986. *Remote Sensing Digital. Image Analysis: An Introduction.* Springer-Verlag, New York.

Ritchie, J.C., F.R. Schiebe and J.R. McHenry, 1976. "Remote sensing of suspended sediments in surface waters." *Photogrammetric Engineering and Remote Sensing* . 42(12).

Rock, B.N., T. Hoshizaki and J.R. Miller, 1988. "Comparison of *in situ* and airborne spectral measurements of the blue shift associated with forest decline." *Remote Sensing of the Environment* 24(1).

Rowan, K.S., 1989. *Photosynthetic pigments of algae*. Cambridge University Press, New York.

Sathyendranath, S., L. Prieur and A. Morel, 1989. "A three component model of ocean colour and its application to remote sensing of phytoplankton pigments in coastal water." *International Journal of Remote Sensing* 10(8).

Scagel, R.F., 1967. *Guide to Common Seaweeds of British Columbia*. British Columbia, Queens Printers.

Smith, R.C. and K.S. Baker, 1981. " Optical properties of the clearest natural waters (200 - 800 nm)." *Applied Optics* 20.

Snively, G., 1983. *Exploring the Seashore in British Columbia, Washington and Oregon* . Gordon Soules Book Pub. Ltd.,Vancouver.

Specht, M.R., D. Needles and N.L. Fritz, 1973. "New color film for water photography penetration." *Photogrammetric Engineering and Remote Sensing* 39(4)

Stanez, K. 1992. "A decade of imaging spectrometry in Canada." *Canadian Journal of Remote Sensing* 18(4).

Stewart, R.H., 1985. *Methods of Satellite Oceanography*. University of California Press, Los Angeles.

Sutherland, I.R., 1989, "Kelp inventory, 1988 Juan De Fuca Strait." *Fisheries Development Report No. 35*. Ministry of Agriculture and Fisheries, Province of British Columbia.

Tassan, S., 1988, "The effect of dissolved 'yellow substance' on the quantitative retrieval of chlorophyll and total suspended sediment concentrations from remote measurements of water colour." *International Journal of Remote Sensing* 9(4).

Thompson, L.L., 1979. "Remote sensing using solid state array technology." *Photogrammetric Engineering and Remote Sensing* 45.

Tou, J.T. and R.C. Gonzlaes, 1974. *Pattern Recognition Principles*. Addison-Wesley Publishing Co.

Tucker, C.J. and L.D. Miller, 1977. "Soil spectra contributions to grass canopy spectral reflectance." *Photogrammetric Engineering and Remote Sensing* . 43(6).

Vadas, R.L. and F.E. Manzer, 1971. "The use of aerial color photography for studies on rocky intertidal benthic marine algae." *Aerial Color Photography in the Plant Sciences and Related Fields: Proceedings of the Third Biennial. Workshop on Aerial Color Photography in the Plant Sciences.*

Vane, G. A.F.H. Goetz and J.B. Wellman, 1984. "Airborne imaging spectrometer: a new tool for remote sensing." *IEEE Transactions on Geoscience and Remote Sensing* 22(6).

Wertheim, A., 1984. *The Intertidal Wilderness*. Sierra Club Books, San Francisco .

Williams, J., 1970. *Optical Properties of the Sea*. United States Naval Institute, Annapolis Maryland.

Wiltens, J., U. Schreiber and W. Vidaver, 1978. "Chlorophyll fluorescence induction: an indicator of photosynthetic activity in marine algae undergoing desiccation." *Canadian Journal of Botany* 56.

Yost, E. and S. Weneroth, 1968. "Coastal penetration using multispectral photographic techniques." *Proceedings of the Fifth Symposium on Remote Sensing and the Environment..*

Zibordi, G., F. Parmiggiani and L. Albertotanza, 1990. "Application of aircraft multispectral scanner data to algae mapping over the Venice Lagoon." *Remote Sensing of the Environment* 34.

Zibordi, G.F., G. Maracci and P. Schlittenhardt, 1990. "Ocean colour analysis in coastal waters by airborne sensors." *International Journal of Remote Sensing* 11(5).

Appendix A

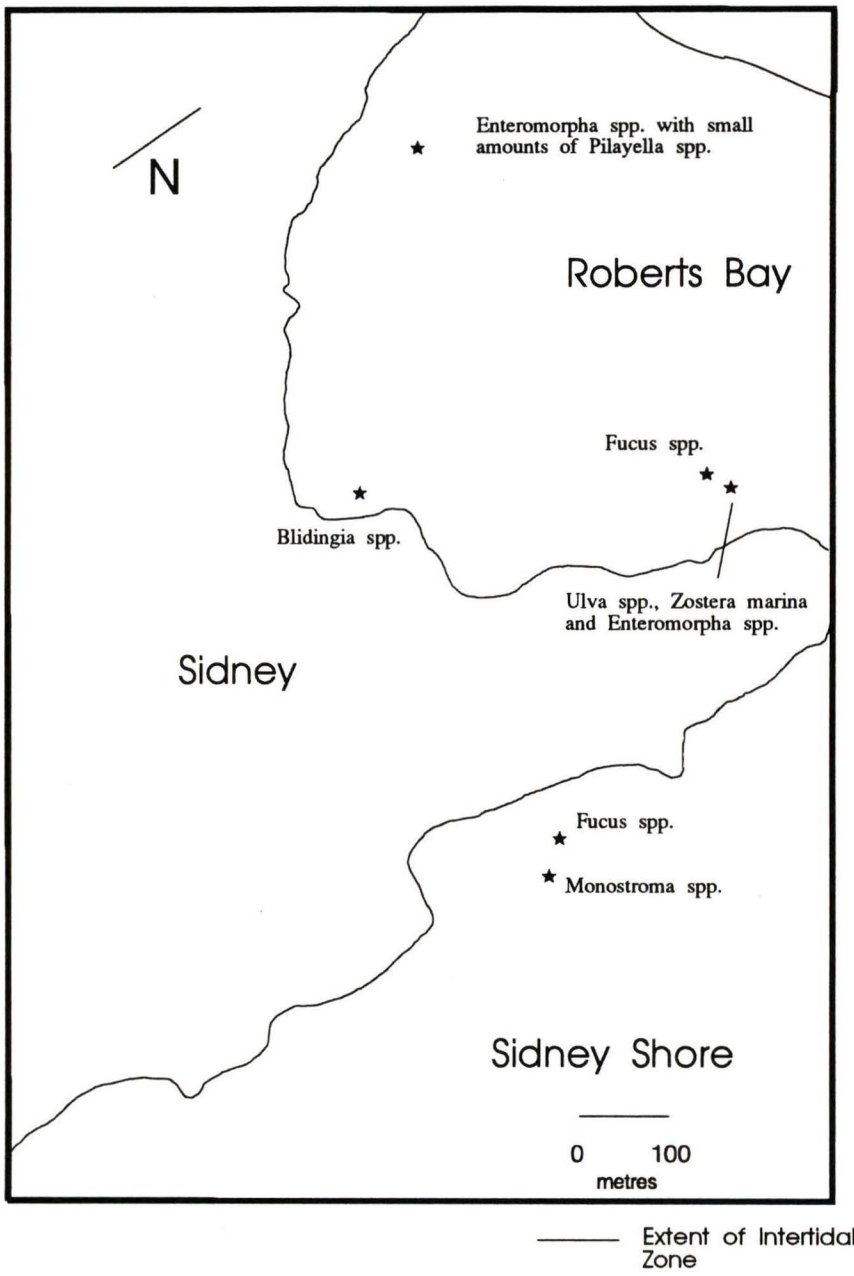

Locations of study sites and species recorded at study sites for Roberts Bay and Sidney Shore

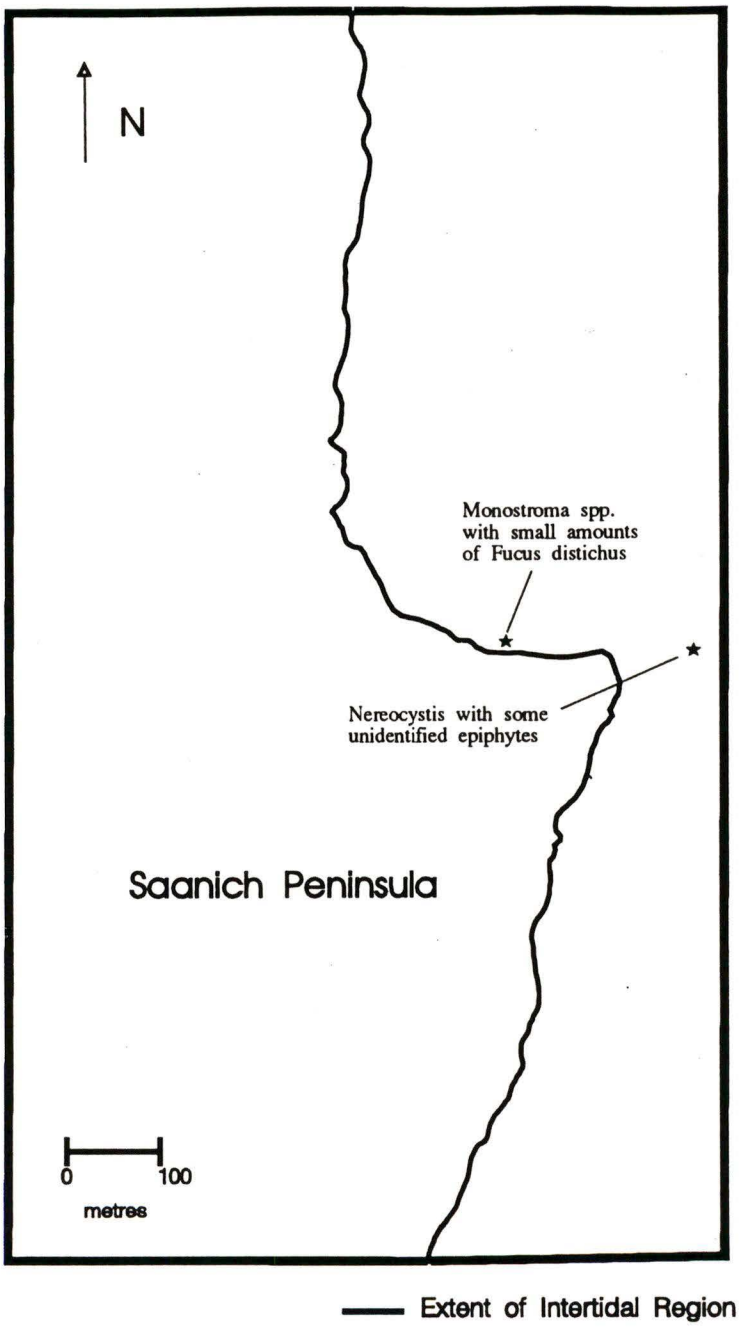

Locations of study sites and species recorded at study sites for Island View Beach.

VITA

Surname: Zacharias Given Names: Mark Abe

Place of Birth: Montreal, Canada Date of Birth: Aug 22 1967

Educational Institutions Attended

University of Victoria	1987 - 1993
Trinity Western University	1986 - 1987
East Kootenay Community College	1985 - 1986

Degrees Awarded

B. Sc. (Honours)	1991

Publications

Zacharias, M., O. Niemann and G.A. Borstad. 1992. "An assessment and classification of a multispectral bandset for the remote sensing of intertidal seaweeds." Canadian Journal of Remote Sensing Vol. 18 No. 4.

PARTIAL COPYRIGHT LICENSE

I hereby grant the right to lend my thesis to users of the University of Victoria Library, and to make single copies only for such users or in response to a request from the Library of any other university, or similar institution, on behalf or for one of its users. I further agree that permission for extensive copying of this thesis for scholarly purposes may be granted by me or a member of the University designated by me. It is understood that copying or publication of this thesis for financial gain shall not be allowed without my written permission.

Title of Thesis: Mapping Coastal Habitats using an Imaging Spectrometer

Author [redacted]

Mark Zacharias

April 22 1993